

Journal Pre-proof

From inactivation to intervention: X chromosome silencing in disease pathogenesis and emerging therapeutic strategies

Yuan Fu, Xuling Tan, Lixia Qin, Chunyu Wang



PII: S2352-3042(25)00453-2

DOI: <https://doi.org/10.1016/j.gendis.2025.101964>

Reference: GENDIS 101964

To appear in: *Genes & Diseases*

Received Date: 13 April 2025

Revised Date: 27 September 2025

Accepted Date: 8 October 2025

Please cite this article as: Fu Y, Tan X, Qin L, Wang C, From inactivation to intervention: X chromosome silencing in disease pathogenesis and emerging therapeutic strategies, *Genes & Diseases*, <https://doi.org/10.1016/j.gendis.2025.101964>.

This is a PDF of an article that has undergone enhancements after acceptance, such as the addition of a cover page and metadata, and formatting for readability. This version will undergo additional copyediting, typesetting and review before it is published in its final form. As such, this version is no longer the Accepted Manuscript, but it is not yet the definitive Version of Record; we are providing this early version to give early visibility of the article. Please note that Elsevier's sharing policy for the Published Journal Article applies to this version, see: <https://www.elsevier.com/about/policies-and-standards/sharing#4-published-journal-article>. Please also note that, during the production process, errors may be discovered which could affect the content, and all legal disclaimers that apply to the journal pertain.

© 2025 Publishing services by Elsevier B.V. on behalf of KeAi Communications Co. Ltd.

1 **From inactivation to intervention: X chromosome silencing in disease**
2 **pathogenesis and emerging therapeutic strategies**

3

4 Yuan Fu^{a,b,f}, Xuling Tan^{a,b,e,f}, Lixia Qin^{b,d}, Chunyu Wang^{a,b,c,e,*}

5

6 ^a *Department of Medical Genetics, The Second Xiangya Hospital of Central South*
7 *University, Changsha, Hunan 41001, China*

8 ^b *Department of Neurology, The Second Xiangya Hospital of Central South University,*
9 *Changsha, Hunan 41001, China*

10 ^c *Key Laboratory of Hunan Province in Neurodegenerative Disorders, Central South*
11 *University, Changsha, Hunan 41001, China*

12 ^d *Clinical Medical Research Center for Stroke Prevention and Treatment of Hunan*
13 *Province, Department of Neurology, The Second Xiangya Hospital of Central South*
14 *University, Changsha, Hunan 41001 China*

15 ^e *Department of Medical Genetics, Hunan Province Clinical Medical Research Center*
16 *for Genetic Birth Defects and Rare Diseases, The Second Xiangya Hospital of Central*
17 *South University, Changsha, Hunan 41001, China*

18

19 ^{*} Corresponding author. Department of Neurology, The Second Xiangya Hospital,
20 Central South University, Changsha, Hunan 410011, China.

21 *E-mail address:* wangchunyu@csu.edu.cn (C. Wang).

22 Peer review under responsibility of Chongqing Medical University.

23 ^f These authors contributed equally to this work.

24

25 Abstract

26 X chromosome inactivation (XCI) is a crucial epigenetic mechanism that balances
27 X-linked gene expression in females via random silencing of one X chromosome.
28 Skewed XCI—non-random inactivation favoring one allele—impacts disease
29 penetrance in X-linked disorders. In heterozygous females, phenotypic severity
30 correlates with XCI skewing degree. Accurate XCI quantification is critical for
31 predicting clinical variability and improving risk assessment in X-linked mutation
32 carriers. The X inactivation-specific transcript (*Xist*) gene drives XCI initiation
33 through its long non-coding RNA (lncRNA) that recruits polycomb repressive
34 complexes 2 (PRC2) to establish stable heterochromatin. Bracingly, emerging
35 therapies leveraging XCI reactivation (*e.g.*, *Xist* RNA inhibition, *Xist* RNA epigenetic
36 modification) show preclinical potential to rescue silenced alleles, advancing
37 treatment strategies for X-linked diseases. This review synthesizes XCI mechanisms,
38 current skewing detection methods, and therapeutic developments, providing a
39 roadmap for clinical translation of XCI-targeted interventions.

40

41 **Keywords:** Detection of X chromosome inactivation; Mechanisms; The inactive X
42 chromosome reactivation; Therapeutic strategies; X chromosome inactivation

43

44 Introduction

45 In 1949, cytogeneticists Murray Barr and Ewart Bertram made a seminal discovery using
46 Feulgen staining: they identified a distinct chromatin body adjacent to the nuclear

47 envelope in female cat neurons, which was conspicuously absent in male specimens.¹
48 This dense, drumstick-shaped structure, subsequently termed the Barr body, became
49 recognized as the cytological manifestation of X chromosome inactivation (XCI). By
50 1960, Susumu Ohno proposed that mammals exhibit two distinct forms of the X
51 chromosome: one resembling transcriptional activity of an autosome, and the other
52 adopting a condensed, heterochromatic state, corresponding to the Barr body.² This
53 foundational work culminated in Mary F. Lyon's groundbreaking 1961 hypothesis, which
54 established three pivotal principles: i) random inactivation of one X chromosome in
55 female somatic cells during embryogenesis, ii) irreversible heterochromatinization of the
56 inactivated X, and iii) clonal propagation of this epigenetic state, thereby achieving
57 dosage equilibrium between XY males and XX females.³

58
59 XCI is a critical mechanism in female mammals for balancing the dosage of X-linked
60 genes, ensuring equivalent gene expression between males and females through randomly
61 silencing one X chromosome during early embryogenesis.⁴ This process is regulated by
62 the long non-coding RNA (lncRNA) gene X inactivation-specific transcript (*Xist*).⁵

63 As the master regulator of XCI, *Xist* resides within the X-inactivation center (XIC),
64 making its functional characterization essential for deciphering XCI mechanisms.

65
66 Originally recognized for its role in dosage compensation, XCI is now understood to have
67 broader biological implications. Skewed XCI, where one X chromosome is preferentially
68 inactivated, contributes to phenotypic variability in X-linked disorders, correlating with
69 disease severity. Consequently, female patients with the same mutation may display

70 different disease severities due to varying degrees of X chromosome skewing.⁶ It was
71 previously believed that once XCI is established, deletion of *Xist* or the entire XIC in
72 somatic cells would not lead to observable reactivation of the inactive X chromosome
73 (Xi).⁷ However, with technological advancements, it has been shown that conditional
74 deletion of *Xist* can result in the reactivation of individual genes on the Xi.⁸ These
75 insights have propelled XCI modulation into therapeutic focus, with two emerging
76 strategies showing promise: i) Reactivation of the Xi to restore gene expression, and ii)
77 Correction of skewed XCI patterns to mitigate clinical heterogeneity.

78
79 Recent studies on skewed XCI and its association with X-linked phenotypes are
80 advancing. While most research on XCI reactivation as a potential therapeutic strategy
81 has focused on Rett syndrome (RTT), some studies have also investigated other
82 conditions, such as X-linked sideroblastic anemia (XLSA). However, considerable
83 challenges remain before these findings can be applied in clinical practice. First and
84 foremost, it is crucial to elucidate the mechanisms governing the initiation and
85 maintenance of XCI in humans, as this will provide a robust foundation for future
86 therapeutic advancements. Additionally, accurately quantifying the skewing ratio of XCI
87 is essential for developing personalized treatment strategies.

88
89 This review systematically examines four critical domains: i) Molecular mechanisms
90 underlying XCI; ii) Impact of XCI skewing on phenotypic variability in X-linked
91 diseases; iii) Technological evolution in XCI assessment; iv) Translational applications of
92 XCI modulation.

93

94 **Mechanism of inactivation of the X chromosome: *Xist* locus**

95 In mice and humans, the XIC is a genomic region on the X chromosome responsible for
96 initiating XCI.^{9,10} In 1991, the *Xist* gene, a novel X-linked gene exclusively expressed
97 from the Xi, was identified within the XIC as being central to XCI.⁵ Subsequent
98 comparative analyses demonstrated that *Xist* is evolutionarily conserved in both sequence
99 composition and genomic organization across mammalian species.^{11,12}

100

101 Although XCI is conserved in female mammals, its early silencing mechanisms exhibit
102 marked divergence between rodents and primates.¹³ In humans, both X chromosomes
103 undergo transcriptional dampening rather than complete inactivation during the early
104 pre-implantation embryo stage. *XIST* is expressed from both X chromosomes to ensure
105 early dosage compensation at the blastocyst stage.¹⁴ The lncRNA X active- specific
106 transcript (XACT) transiently co-expresses with *XIST*.¹⁵ XACT is an X-linked
107 transcriptional unit spanning over 250 kb, located approximately 50 Mb distal to *XIST*. It
108 is identified in humans and conserved among great apes, but absent in lesser apes and
109 more distantly related species.¹⁶ However, recent studies using naive human embryonic
110 stem cells indicate that XACT does not significantly regulate *XIST* expression,
111 localization, or function, nor does it influence X-linked gene expression during the
112 pre-implantation stage, suggesting XACT is dispensable for X chromosome
113 transcriptional regulation at this stage.¹⁷ Random X-chromosome inactivation (rXCI)
114 occurs only at the late blastocyst stage.¹³ In mice, imprinted X-chromosome inactivation
115 (iXCI) occurs, specifically silencing the paternal X chromosome (Xp).¹⁸ After

116 fertilization, both maternal and paternal X chromosomes are initially active. iXCI is
117 initiated at the four-cell stage, and by embryonic day 3.5 (E3.5), all embryonic cells have
118 an inactive Xp.¹⁹ Xp remains inactive in extraembryonic tissues but is reactivated in the
119 inner cell mass during the blastocyst stage. Similar to humans, rXCI occurs at the late
120 blastocyst stage (Fig. 1A).^{20,21}

121

122 Given that it is coated by *Xist* RNA, the X chromosome undergoes gene silencing. Most
123 research investigating the mechanisms driving XCI has relied on dissecting the function
124 of *Xist* RNA itself. In mice, *Xist* RNA is structurally organized into multiple Repeat
125 modules (A–F),¹¹ which act as functional modules during XCI (Fig. 1B).²² These
126 modules interact with chromatin modifiers and spatial organization factors, playing
127 essential roles in establishing and maintaining the silenced state of the Xi.

128

129 The Repeat A module (nucleotides 335–700 of *Xist*), the most evolutionarily conserved
130 RNA domain, is indispensable for Xi-wide transcriptional silencing of nearly all genes on
131 the Xi. Interacting with Repeat A via its RNA recognition motifs (RRMs),²³ SPlit ENds
132 (SPEN), a ribonucleoprotein (RBP) containing an SPEN paralogue/orthologue C-terminal
133 (SPOC) domain, is recruited to active promoters and enhancers across the X chromosome,
134 initiating gene silencing,²⁴ and further mediates the recruitment of chromatin-modifying
135 complexes to promote histone H3/H4 deacetylation and hinder RNA polymerase II (Pol
136 II) loading.^{25,26} Meanwhile, the SPOC domain of SPEN is involved in the recruitment of
137 several repressor complex members of NR corepressor (NCoR), the silencing mediator of
138 retinoic acid or thyroid hormone receptor (SMRT), and nucleosome remodeling

139 deacetylase (NuRD) complex.²⁴ SPEN potentially activates part of the histone
140 deacetylase 3 (HDAC3) population pre-bound to the Xi enhancer by delivering
141 NCoR/SMRT complex members, leading to histone deacetylation and facilitating histone
142 3 lysine 4 monomethylation (H3K4me1) demethylation.²⁷ Additionally, Repeat A recruits
143 other SPOC-containing proteins, such as RNA-binding motif protein 15 (RBM15) and
144 15B (RBM15B), which facilitate gene silencing through N⁶-methyladenosine (m⁶A)
145 RNA methylation.²⁸ The m⁶A is deposited along the m⁶A hotspot in the downstream *Xist*
146 transcript located in the Repeat A region. This modification is subsequently recognized
147 and bound by the m⁶A reader YTH domain-containing 1 (YTHDC1).^{29,30}
148
149 The Repeat B module (nucleotides ~2850–3050) and the Repeat C module (nucleotides
150 ~2850–3050) are responsible for maintaining the transcriptionally silent state of the Xi.
151 After the initial establishment of silencing by the Repeat A/SPEN module, the B/C
152 Repeat modules recruit polycomb group (PcG) protein complexes to the Xi.³¹ Among
153 these complexes, polycomb repressive complexes 1 (PRC1) and 2 (PRC2) are essential in
154 *Xist*-mediated chromosomal silencing.³² PRC1 and PRC2 function in an independent yet
155 complementary manner during the maintenance phase of XCI, with PRC1 mediating the
156 silencing of CpG island (CGI)-associated genes via histone H2A lysine 119
157 mono-ubiquitination (H2AK119ub1), and PRC2 targeting a distinct or partially
158 overlapping set of genes through histone H3 lysine 27 trimethylation (H3K27me3),
159 thereby cooperatively ensuring stable silencing of the Xi in extra-embryonic tissues.³³
160 The B/C Repeat modules, enriched in cytosine residues, are recognized by heterogeneous
161 nuclear ribonucleoprotein K (HNRNPK).³⁴ HNRNPK recruits the PCGF3/5-PRC1

162 complex, which catalyzes H2A lysine 119 ubiquitination (H2AK119ub), a chromatin
163 modification marking silenced regions.^{32,35} Additionally, Jarid2, a PRC2 cofactor,
164 recognizes H2AK119ub and facilitates PRC2 recruitment to the Xi, further reinforcing
165 heterochromatin formation.³⁶

166
167 The Repeat E module (nucleotides ~10,275–11,400) mediates interactions with multiple
168 proteins to anchor *Xist* RNA to the Xi, playing a critical role in maintaining XCI.
169 CDKN1A-interacting zinc finger protein 1 (CIZ1) facilitates the association of *Xist* with
170 the nuclear matrix in a cell lineage-specific manner.^{37,38} Additionally, four proteins,
171 polypyrimidine tract-binding protein 1 (PTBP1), Matrin 3 (MATR3), TAR DNA-binding
172 protein 43 (TDP-43), and CUGBP Elav-like family member 1 (CELF1), directly interact
173 with the Repeat E module, forming a CIZ1-independent complex. This complex
174 stabilizes *Xist* RNA coating on the Xi, after the transcriptional silencing initiated by the
175 Repeat A module and PcG recruitment mediated by the Repeat B/C modules.³⁹

176
177 The roles of the Repeat D and F modules are less well understood. Genetic ablation of the
178 Repeat D module appears to have no discernible impact on *Xist* RNA coating of the Xi or
179 PcG protein recruitment.³⁵ In contrast, deletion of the Repeat F module disrupts *Xist*
180 RNA stability, leading to failure in transcriptional silencing.^{35,40,41}

181
182 The Repeat elements within the human *XIST* gene are relatively conserved compared
183 with their counterparts in mice, albeit with notable differences. In humans, the B Repeat
184 is split into two distinct segments, termed Bh and B. Additionally, the extent of Repeat

185 expansion varies between species. Notably, the C Repeat is substantially expanded in
186 mice, a feature that appears to be rodent-specific, whereas in humans it is reduced to a
187 single monomeric unit. In contrast, the D Repeat exhibits a marked expansion in human
188 *XIST* but predominantly consists of truncated monomers in the rodent lineage.⁴² Despite
189 these sequence divergences, the higher-order folding of *Xist* RNA is conserved between
190 mice and humans, partitioned into five major structural modules: Repeat A, F, B/C/D, E,
191 and exon 6/7. The E Repeat is located at the 5' end of exon 6 of *XIST/Xist* and at the 5' end
192 of exon 7 of *XIST/Xist*, respectively; all other Repeats are contained within the large first
193 exon of *XIST/Xist*.^{30,43}

194
195 Mouse models have long served as the primary system for studying XCI in mammals and
196 have been instrumental in elucidating the role of *Xist* in gene silencing. During XCI,
197 specific Repeat modules and structural motifs in *Xist* RNA from mouse embryonic stem
198 cells recruit chromatin remodelers and transcriptional repressors, driving chromatin
199 compaction and gene silencing.^{44,45} During *Xist* transcription, *Xist* RNA accumulates at
200 discrete "entry sites" on the X chromosome destined for inactivation, subsequently
201 spreading to distal genomic regions to form a contiguous RNA coating.⁴⁶ This
202 RNA-mediated coating coincides with chromatin structural reorganization, marking the
203 onset of XCI.

204
205 During the maintenance phase of XCI, late-stage epigenetic modifications include the
206 specific enrichment of the histone variant macroH2A on the Xi,⁴⁷ DNA methylation of
207 CpG islands by DNA (cytosine-5)-methyltransferase 3B (DNMT3B),⁴⁸ and histone H3

208 lysine 9 dimethylation (H3K9me2). H3K9me2 facilitates the recruitment of the
209 chromodomain Y-like (CDYL)–G9A–MAX gene-associated (MGA) complex, which
210 may, in turn, promote the propagation of H3K9me2 across the Xi.⁴⁹ However, the precise
211 roles of these late-stage epigenetic modifications in the maintenance of XCI, as well as
212 their dependency on *XIST* RNA, remain unclear.

213

214 Ultimately, the assembly of *Xist*-scaffolded protein complexes at the Xi locus initiates a
215 cascade of events—silencing initiation, spreading, and maintenance—culminating in the
216 establishment of a repressive chromatin state and three-dimensional chromosomal
217 restructuring.

218

219 **Regulatory networks controlling *Xist* expression**

220 Up-regulation of *Xist* is essential for initiating XCI. The *Xist* antisense non-coding
221 transcription unit *Tsix* is the first and most prominent negative regulator of *Xist*.⁵⁰ *Tsix*
222 suppresses ectopic expression of *Xist* on the maternal X chromosome; mutations in *Tsix*
223 disrupt this suppression, leading to abnormal *Xist* up-regulation. Chromosome
224 conformation capture studies of the XIC show that this locus is divided into at least two
225 topologically associating domains (TADs): the *Xist* TAD and *Tsix* TAD (Fig. 1C).⁵¹
226 Within these domains, intra-domain chromatin interactions are more frequent than
227 inter-domain contacts.⁵² The *Xist* promoter is located within the *Xist* TAD, which also
228 contains several positive regulatory elements, including the proximal non-coding genes
229 *Jpx* and *Ftx*, the ring finger protein 12 (RNF12) gene (*Rnf12*),^{53,54} and the *Xist*-enhancing
230 regulatory transcript (*Xert*), all of which are up-regulated during cellular differentiation.

231 In contrast, the *Tsix* TAD contains the Xite enhancer for *Tsix*⁵⁵ and the long non-coding
232 RNA *Linx*, which acts as a distal cis-acting repressor of *Xist*.¹⁰
233
234 *Xist* and *Tsix* are localized at the boundary between two TADs.⁵⁵ *Jpx*, located 10 kb
235 upstream of the *Xist* locus, acts as a trans-activator of *Xist* through both cis- and
236 trans-acting mechanisms. It activates *Xist* by displacing CCCTC-binding factor (CTCF),
237 an RNA-binding protein that represses *Xist* transcription.⁵⁶ *Ftx*, another upstream
238 non-coding RNA locus, acts as a cis-acting regulatory element. In human cellular models,
239 a 453 kb deletion overlapping *Jpx* and *Ftx* causes skewed *Xist* expression on the intact X
240 chromosome.⁵⁷ The *Xert* locus, approximately 200 kb upstream of *Xist*, is
241 co-up-regulated with *Jpx* and *Ftx* during cellular differentiation. The *Xert* promoter
242 (*XertP*) and *Xert* enhancer cluster (*XertE*) enhance *Xist* transcriptional activity and also
243 elevate *Ftx* expression through cis-regulatory interactions.⁵³
244
245 In addition to these non-coding elements, the *Xist* TAD also harbors the *Rnf12* gene,
246 which encodes an E3 ubiquitin ligase. RNF12 acts as a dose-dependent trans-activator of
247 *Xist*,⁵⁸ promoting the proteasomal degradation of the pluripotency transcription factor
248 REX1 (also known as zinc finger protein 42 or ZFP42). During cellular differentiation,
249 REX1 degradation facilitates *Xist* up-regulation and initiates XCI.⁵⁹ RNF12 also
250 synergistically interacts with the cis-regulatory regions of *Jpx* and *Ftx*.⁶⁰ Furthermore, the
251 autosomal trans-activator Yin Yang 1 (YY1) competes with REX1 for binding to the 5'
252 region of *Xist*, thereby activating its promoter.⁶¹ Recent studies have identified YY1 as a
253 key gene-intrinsic regulatory factor in XCI, whereby its binding at promoters and

254 enhancers of slow-silencing genes serves to delay the progression of *Xist*-mediated gene
255 silencing.⁶²

256

257 The *Tsix* transcript originates ~15 kb downstream of *Xist*, partially overlapping its locus
258 and transcribed in the antisense orientation. The long non-coding RNA *Linx*, located
259 ~150 kb upstream of the *Xite* enhancer, facilitates *Xist* transcriptional activation and XCI
260 initiation through its promoter *LinxP*.^{63,64}

261

262 In contrast to murine *Tsix*, human *TSIX* does not fully overlap with the *XIST* locus and is
263 co-expressed with *XIST* from the Xi, challenging its proposed role as a transcriptional
264 repressor of *XIST*.^{65,66} Consistent with this, the *TSIX* TAD, aside from the *LinxP* element,
265 shows limited conservation compared with the highly conserved *XIST* TAD.⁶⁴

266

267 In humans, *JPX* and *FTX* are conserved within the same TAD as *XIST*, yet exhibit
268 pronounced functional divergence between species that is not explained by primary
269 sequence conservation. While the function of *FTX* is not conserved in humans, *JPX*
270 serves as a key regulator of *XIST* expression in both humans and mice. Importantly,
271 unlike in mice, human *XIST* expression is regulated by the transcriptional activity of *JPX*
272 rather than the accumulation of *JPX* RNA.⁵⁴ These findings underscore the remarkable
273 functional plasticity of conserved lncRNA loci within the regulatory architecture of XCI.

274

275 **X chromosome inactivation and phenotypic manifestations of X-linked disorders**

276 In humans, XCI initiates during the early stages of embryonic implantation. The selection
277 of which X chromosome—maternal (X_m) or X_p—is to be inactivated is traditionally
278 considered a random process, with both parental chromosomes having equal probability
279 of being silenced.⁶⁷ Under purely random conditions, the expected ratio of maternal to
280 paternal XCI is 1:1 (50:50). However, deviations from this expected ratio result in
281 skewed XCI. Extreme skewing occurs when $\geq 90\%$ or $\geq 95\%$ of cells inactivate the
282 same X chromosome. In the general female population, XCI patterns exhibit considerable
283 variability, ranging from highly skewed (0:100, where one X chromosome remains active
284 in all cells) to balanced (50:50, where both X chromosomes are equally active across
285 cells).^{68,69} This variability underscores the stochastic nature of XCI and its contribution to
286 phenotypic diversity in females.⁷⁰

287
288 Previous studies have shown a correlation between skewed XCI and phenotypic
289 variability in female carriers of X-linked disorders. The expression of pathogenic alleles
290 can influence the clinical manifestations in female carriers of X-linked mutations,
291 explaining the observed variability in clinical presentations among affected individuals.
292 Several X-linked disorders exhibit non-random XCI, such as Fabry disease, Duchenne
293 muscular dystrophy,⁷¹ hemophilia, Becker muscular dystrophy, and X-linked chronic
294 granulomatous disease (Table 1). In this section, we focus on RTT, a well-characterized
295 X-linked disorder, to illustrate how XCI skewing impacts disease phenotypes.

296
297 RTT is a rare neurodevelopmental disorder that predominantly affects females.¹⁰⁰

298 Affected individuals typically experience normal development during the first 6–18

299 months of life, followed by developmental plateauing, regression of acquired speech and
300 motor skills, stereotypic hand movements, gait abnormalities, and aberrant respiratory
301 patterns. As the disorder progresses, individuals often experience severe intellectual
302 disability, epilepsy, and profound impairments in social and communicative abilities.
303 RTT is caused by mutations in the X-linked methyl-CpG-binding protein 2 (*MECP2*)
304 gene, which encodes a transcriptional regulator critical for brain development.¹⁰¹
305 Approximately 90%–95% of classic RTT cases and 70% of atypical cases harbor
306 *MECP2* mutations. As *MECP2* is subject to XCI, phenotypic variability in female
307 carriers is heavily influenced by XCI skewing. In females with a heterozygous *MECP2*
308 mutation, random XCI theoretically results in 50% of cells expressing the wild-type allele
309 and 50% expressing the mutant allele. However, skewed XCI, where the mutant *MECP2*
310 allele is preferentially inactivated in most cells, can reduce clinical severity or even lead
311 to asymptomatic carrier status. Conversely, preferential inactivation of the wild-type
312 allele exacerbates disease manifestations. Thus, the degree of XCI skewing directly
313 correlates with the clinical heterogeneity observed in RTT (Fig. 2).
314
315 Most *de novo* mutations in the *MECP2* gene occur on the paternal allele,^{102–104} leading to
316 exclusive transmission to female offspring. A study by Knudsen et al examined the
317 parental origin of the Xi in RTT individuals and observed that in cases with skewed XCI,
318 the paternally derived X chromosome (carrying the mutant *MECP2* allele) was
319 preferentially inactivated. This finding suggests that individuals with highly skewed XCI
320 patterns exhibit a reduced proportion of cells expressing the mutant *MECP2* allele,
321 potentially attenuating disease severity.¹⁰⁵ While the majority of RTT cases are sporadic,

322 unaffected mothers harboring *MECP2* pathogenic variants have been reported.¹⁰⁶ These
323 carriers are likely protected by extreme XCI skewing, where the X chromosome carrying
324 the mutant allele is predominantly silenced, minimizing its expression in critical tissues.
325

326 Despite extensive research, conflicting evidence persists regarding the correlation
327 between XCI skewing and phenotypic severity in RTT. In a study by Huppke et al, three
328 female carriers of *MECP2* mutations exhibited mild phenotypes despite their genetic
329 status, with XCI skewing ratios of 84:16, 95:5, and 76:24, favoring inactivation of the
330 mutant allele. This observation supports the hypothesis that skewed XCI attenuates
331 disease severity by reducing mutant allele expression.¹⁰⁷ Similarly, L. Villard reported an
332 asymptomatic female carrier with extreme XCI skewing whose daughter presented with
333 classic RTT. This illustrates that while skewed XCI in carriers does not prevent the
334 transmission of the mutation, it can modulate phenotypic expression in offspring.¹⁰⁸

335 Additionally, Hayley Archer et al further showed that RTT patients with *MECP2*
336 mutations (p.R168X and p.T158M) exhibited increased clinical severity that correlated
337 with a higher proportion of cells expressing the mutant allele. This aligns with findings
338 that milder RTT cases are associated with greater XCI skewing toward mutant allele
339 inactivation, though parental origin of the mutation was not determined in this study.¹⁰⁹

340 Contrastingly, a large-scale analysis by Xiaolan Fang et al of 320 RTT cases and
341 maternal blood samples revealed nuanced relationships between XCI skewing and
342 clinical severity. In classic RTT patients with preferential inactivation of the maternally
343 derived allele, a weak positive correlation ($r_s = 0.35$, $n = 40$) was observed between XCI
344 skewing ratios and Clinical Severity Score (CSS). However, no such correlation ($r_s = -$

345 0.06, $n = 180$) was found in patients with paternal allele-predominant XCI skewing.¹¹⁰
346 These findings highlight the complexity of XCI-phenotype interactions, which may
347 depend on mutation origin, tissue-specific skewing, or modifier genes. The latest study of
348 Duchenne muscular dystrophy also showed different and contradictory results than
349 before.¹¹¹
350
351 To reliably assess the impact of XCI skewing on phenotypic variability, future studies
352 should focus on familial cohorts with identical *MECP2* mutations to minimize
353 confounding effects due to mutation-specific variability. Additionally, rigorous
354 quantification of phenotypic severity using standardized metrics, such as clinical severity
355 scores, is essential for establishing robust phenotypic correlations. The tissue type
356 analyzed also significantly affects findings. Most studies evaluate XCI skewing in easily
357 accessible somatic cells (*e.g.*, leukocytes, buccal epithelial cells, urinary cells), rather
358 than affected tissues like brain cells. However, lineage-specific XCI skewing, driven by
359 differences in embryonic origin, may result in divergent inactivation patterns across
360 tissues in the same individual.¹¹² Age-related dynamics in XCI skewing further
361 complicate interpretations, as skewing ratios may evolve over time.¹¹³ While analyzing
362 affected tissues (*e.g.*, neurons) provides the most clinically relevant insights, this requires
363 invasive biopsies and poses ethical concerns. Additionally, longitudinal studies are
364 needed to address age-dependent phenotypic progression, as young patients may exhibit
365 delayed symptom onset, which complicates cross-sectional analyses. Finally, beyond XCI
366 skewing, other mechanisms, including germline mosaicism and epigenetic modifiers,
367 may also contribute to phenotypic variability.⁷⁷ A multi-factorial approach integrating

368 genetic, epigenetic, and environmental factors is necessary to fully understand the
369 determinants of X-linked disorders' severity.

370

371 **Quantitative detection of XCI ratio**

372 Since the initial observation of XCI, methodologies for detecting and quantifying XCI
373 patterns have evolved significantly. Quantitative assessment of XCI is essential for
374 understanding phenotypic diversity in females and evaluating disease risks associated
375 with X-linked mutations. By determining whether XCI occurs randomly or in a skewed
376 manner, researchers can elucidate its impact on X-linked gene expression and clinical
377 manifestations, thereby aiding in the assessment of symptom severity in carriers of
378 X-linked disorders. Furthermore, XCI-based therapeutic strategies—most notably Xi
379 reactivation—are currently under active investigation. Before clinical implementation,
380 precise quantification of XCI ratios in patients is necessary to establish baseline
381 inactivation patterns. Therapeutic efficacy depends on achieving precise reactivation
382 thresholds in affected cells and tissues. For instance, reactivating a small proportion (5%–
383 10%) of Xi-linked wild-type *MECP2* alleles may be sufficient to ameliorate symptoms in
384 RTT. Thus, accurate XCI profiling is critical for patient stratification, prediction of
385 therapeutic responsiveness, and monitoring of treatment outcomes.

386

387 **Methylation-based analysis of XCI**

388 During XCI, the Xi undergoes extensive DNA methylation, particularly at CpG islands,
389 while the active X chromosome (Xa) remains largely unmethylated.^{114,115} This epigenetic
390 divergence allows XCI status to be inferred through methylation pattern analysis at

391 specific loci. The human androgen receptor (HUMARA) assay remains the most widely
392 utilized method for XCI analysis. This PCR-based approach employs
393 methylation-sensitive restriction enzymes (*e.g.*, haemophilus parainfluenzae II, HpaII) to
394 target CpG sites in exon 1 of the X-linked Androgen Receptor (*AR*) gene.¹¹⁶
395 Differential methylation between Xi and Xa enables discrimination of parental alleles,
396 where the methylated (undigested) allele corresponds to Xi.

397

398 In addition to *AR*, the X-linked retinitis pigmentosa 2 (*RP2*) gene has been leveraged as
399 an alternative locus for XCI quantification due to its methylation sensitivity.¹¹⁷ Both *AR*
400 and *RP2* contain highly polymorphic repetitive elements adjacent to CpG
401 sites—specifically, a CAG trinucleotide Repeat in *AR* and a GAAA tetranucleotide
402 Repeat in *RP2*—exhibiting high heterozygosity (~0.97) and evolutionary conservation
403 among non-human primates.¹¹⁸ Importantly, as *RP2* lacks known disease associations, it
404 serves as a neutral alternative for XCI studies. Employing a dual *AR/RP2* approach
405 improves the reliability of XCI quantification (Fig. 3A). Parental alleles are distinguished
406 through fragment length analysis (FLA) of PCR-amplified Repeats, which vary in copy
407 number between X chromosomes.¹¹⁹

408

409 Despite its widespread application, the HUMARA assay presents several technical
410 limitations, including PCR artifacts (such as secondary structures or incomplete
411 amplification, which may distort allele size distributions) and fluorescence detection bias
412 (where fluorophore-specific signal quenching or electrophoretic anomalies may
413 compromise haplotype resolution in FLA).

414

415 A more accurate and efficient alternative to restriction enzyme-based methods is bisulfite
416 sequencing, which circumvents the reliance on enzymatic digestion. In this method,
417 sodium bisulfite chemically modifies DNA by converting unmethylated cytosines to
418 uracil, while methylated cytosines remain unchanged. This chemical conversion
419 translates methylation differences into sequence variations, allowing amplification with
420 methylation-specific primers designed to distinguish between methylated and
421 bisulfite-converted (unmethylated) DNA.¹²⁰ By using allele-specific primers and
422 controlled PCR conditions, this approach enhances the precision and reproducibility of
423 amplification outcomes, enabling quantitative assessment of XCI ratios.

424

425 **Advances in XCI profiling: Integrating CRISPR-Cas9 and nanopore sequencing**

426 To mitigate PCR-related biases, a novel strategy known as XCI-ONT integrates
427 CRISPR-Cas9-mediated enrichment of *AR* and *RP2* loci with Oxford Nanopore
428 Technologies (ONT) sequencing to simultaneously assess Repeat length and methylation
429 status. Unlike conventional approaches, XCI-ONT directly interrogates polymorphic
430 Repeats (*e.g.*, *AR* CAG_n and *RP2* GAAA_n) and quantifies methylation at 116 CpG sites in
431 *AR* and 58 CpG sites in *RP2* (Fig. 3B). This method significantly enhances the accuracy
432 of XCI ratio determination by eliminating PCR amplification artifacts and providing
433 high-resolution, long-read methylation data.¹¹⁸

434

435 **RNA-based approaches for XCI assessment**

436 Beyond methylation-based techniques, XCI status can also be assessed at the RNA level.
437 For instance, single-nucleotide polymorphisms (SNPs) in *Xist* RNA have been utilized to
438 distinguish between random and skewed XCI patterns.¹²¹ However, XCI does not operate
439 in isolation; additional factors influencing gene expression, such as cis-regulatory
440 element variations and tissue-specific transcriptional regulators, must also be considered.
441 Consequently, incorporating multiple genes into XCI analyses improves result
442 accuracy.⁹⁷

443
444 With the advent of high-throughput sequencing technologies, RNA sequencing,
445 combined with whole-genome or high-density SNP array data, provides a direct means of
446 quantifying the relative expression of the X_a and X_i . This approach centers on
447 allele-specific expression analysis, which enables precise evaluation of XCI status.
448 Following RNA sequencing, RNA is reverse transcribed into cDNA, and the resulting
449 sequence reads are aligned to a reference genome to identify heterozygous X-linked
450 SNPs. The proportion of reads corresponding to each allele at these SNP loci is then used
451 to calculate the allelic expression ratio.¹²²

452
453 By integrating high-density SNP data, the parental origin (*i.e.*, paternal *vs.* maternal) of
454 allele-specific expression can be resolved. Comparing the average expression ratio of
455 paternal to maternal alleles allows estimation of the XCI ratio, thereby quantitatively
456 delineating the transcriptional activity of each X chromosome (Fig. 3C).

457

458 Advancements in XCI detection and quantification have significantly enhanced our
459 understanding of X-linked gene regulation, phenotypic variation, and disease risk.
460 Methylation-based methods, such as the HUMARA assay and bisulfite sequencing, have
461 long served as foundational tools for XCI analysis, while emerging techniques, such as
462 XCI-ONT, offer improved accuracy and reliability by leveraging long-read sequencing
463 and direct methylation assessment. RNA-based approaches, particularly those
464 incorporating RNA-sequencing and SNP array data, provide complementary insights into
465 X-linked transcriptional dynamics. Collectively, these methodologies are essential for
466 refining XCI profiling, enabling patient stratification in clinical contexts, and facilitating
467 the development of XCI-targeted therapeutic interventions (Table 2).

468

469 **XCI-based therapeutic strategies for X-linked disorders**

470 XCI leads to monoallelic expression of X-linked genes in female cells. In X-linked
471 disorders, pathogenic mutations on the X_a often result in loss of functional protein,
472 driving disease pathogenesis. This suggests that reactivating the X_i to restore expression
473 of the wild-type allele could be a potential therapeutic approach. The feasibility of this
474 approach has been demonstrated in RTT. In RTT mouse models, reactivation of
475 wild-type *Mecp2* expression, even in adult animals, reverses neurological and behavioral
476 deficits, underscoring the potential for phenotypic rescue post-development.¹²³ Thus,
477 targeted reactivation of silenced wild-type alleles on the X_i represents a promising
478 therapeutic avenue for X-linked disorders.

479

480 **Inhibitors of X-chromosome inactivation factors (XCIF)**

481 X-chromosome inactivation factors (XCIFs) are essential for selectively silencing
482 X-linked genes. Recent studies have identified two XCIFs, activin A receptor type I
483 (ACVR1) and 3-phosphoinositide-dependent protein kinase 1 (PDPK1), whose inhibition
484 can reactivate the Xi in differentiated mouse embryonic stem cells. ACVR1 likely
485 maintains *Xist* expression by regulating its transcription and chromatin state, while
486 PDPK1 promotes reactivation of silenced genes by modulating *Xist* RNA localization,
487 stability, and chromatin accessibility.

488

489 ACVR1 is a component of the bone morphogenetic protein (BMP) signaling pathway.
490 Upon BMP signal activation, phosphorylated Sma- and Mad-related proteins (SMAD)
491 enter the nucleus and regulate transcription. When ACVR1 is blocked by drugs, SMAD
492 proteins cannot be phosphorylated and are unable to enter the nucleus. As a result,
493 SMAD cannot bind to the *Xist* promoter region, leading to the suppression of *Xist*
494 transcription. With the inactivation of *Xist*, the previously silenced Xi-*Mecp2* is gradually
495 derepressed and re-expressed. Mechanistic target of rapamycin kinase (mTOR) and
496 serum/glucocorticoid-regulated kinase 1 (SGK1) are two downstream effectors of
497 PDPK1, both of which belong to the PI3K/AKT signaling pathway. YY1 is a key
498 transcriptional activator for the *Xist* promoter, with multiple binding sites. Following the
499 inhibition of mTOR or SGK1, YY1 fails to accumulate at the *Xist* promoter, resulting in
500 transcriptional suppression. Inhibition of mTOR/SGK1 leads to a reduction in Histone H3
501 lysine 4 trimethylation (H3K4me3) levels at the *Xist* promoter, thereby decreasing its
502 activity. Similar to ACVR1 inhibitors, both mTOR and SGK1 inhibitors significantly
503 reduce *Xist* transcripts, resulting in the reactivation of Xi-*Mecp2*.

504

505 In female mouse fibroblast cell lines, shRNA-mediated knockdown of ACVR1 or
506 pharmacological inhibition of PDPK1 reactivated Xi-linked genes, including *MECP2*.¹²⁴
507 Combined treatment with ACVR1 inhibitors and PDPK1 effectors increased *Mecp2*
508 expression and ameliorated morphological deficits in RTT neurons, rescuing somatic cell
509 size and dendritic branching. To precisely quantify Xi-linked *Mecp2* reactivation in the
510 brain, a *Xist* Δ :*Mecp2*/*Xist*:*Mecp2*-GFP mouse model was developed. In this model, the
511 active X chromosome lacks *Xist* and expresses wild-type *Mecp2*, while the inactive X
512 carries a *Mecp2*-GFP fusion reporter (Fig. 4A). Intracerebral injection of the combined
513 inhibitors in female mice resulted in 30% reactivation of Xi-*Mecp2*-GFP in cortical
514 cells.¹²⁵

515

516 However, small-molecule inhibitors may broadly reactivate Xi-linked genes rather than
517 selectively targeting specific loci (*e.g.*, *MECP2*), potentially leading to genomic dosage
518 imbalance. Therefore, optimizing inhibitors to selectively target XCI-related factors is
519 crucial for minimizing off-target effects and ensuring therapeutic safety.

520

521 **Combination of DNA methylation inhibitors (decitabine [5-aza-2-deoxycytidine,**
522 **Aza]) and antisense oligonucleotides (ASOs)**

523 DNA methylation is a key epigenetic modification that maintains XCI, particularly
524 through promoter hypermethylation that enforces gene silencing. ASOs are short
525 synthetic nucleic acid sequences designed to bind specific RNA molecules and disrupt
526 their function. In this context, *Xist*-targeting ASOs bind to *Xist* RNA, blocking its ability

527 to recruit chromatin modifiers and sustain XCI. The combination of DNA methylation
528 inhibitors (*e.g.*, Aza) and *Xist*-targeting ASOs has been explored as a potential approach
529 to reactivate Xi.

530

531 In proof-of-concept experiments, mouse embryonic fibroblasts (MEFs) transfected with a
532 *Mecp2*-luciferase reporter were treated with *Xist* ASOs and Aza. After 5 days, luciferase
533 activity increased by 2.0%–3.5%, reflecting partial reactivation of the Xi-linked *MECP2*
534 allele. Notably, the combined treatment achieved a 30,000-fold up-regulation of *MECP2*
535 expression from the Xi, equating to 2%–5% of normal *MECP2* levels (Fig. 4B). Despite
536 these results demonstrating the feasibility of Xi reactivation, several challenges remain.
537 The modest reactivation efficiency (2%–5%) may be insufficient for clinical benefit, and
538 non-specific effects of Aza (*e.g.*, genome-wide DNA hypomethylation) pose potential
539 safety concerns. Further refinement of ASO specificity and localized delivery methods
540 (*e.g.*, nanoparticles) could enhance therapeutic efficacy while minimizing off-target
541 effects.¹²⁶

542

543 While Aza (decitabine) is FDA-approved for treating acute myeloid leukemia, its
544 systemic toxicity (*e.g.*, myelosuppression) limits its suitability for chronic neurological
545 disorders. Although short-term pulsed regimens may reduce toxicity, the necessity for
546 prolonged, repeated treatments to sustain Xi reactivation remains unclear and warrants
547 further investigation. Additionally, *Xist*-targeting ASOs may inadvertently affect non-*Xist*
548 RNAs or disrupt broader epigenetic regulation. Advanced delivery strategies (*e.g.*, lipid

549 nanoparticles) could enhance ASO bioavailability and neural tissue selectivity, thereby
550 reducing systemic exposure and off-target activity.

551

552 **JAK/STAT pathway inhibitors**

553 The epidermal growth factor receptor (EGFR) exhibits inhibitory activity in certain
554 signaling contexts. A high-throughput luciferase assay in mouse fibroblasts harboring an
555 inactive *MeCP2*-luciferase reporter identified Jaki, a pan-JAK/STAT inhibitor, as a
556 potential Xi reactivator. This screening also revealed that AG490 (a JAK2 kinase
557 inhibitor) and Jaki can reactivate *Mecp2* by suppressing the JAK/STAT pathway,
558 particularly through *Xist* and *Rnf12* down-regulation. The luminescence-based
559 high-throughput screening revealed that a twofold or greater increase in relative
560 luminescence units (RLU) indicates the activation of *Mecp2*. However, in human-hamster
561 hybrid cell lines, AG490 showed weaker *Mecp2* reactivation compared with the robust
562 effects of 5-Aza, suggesting that the effectiveness of JAK/STAT inhibitors may depend
563 on cell type or species-specific regulatory contexts (Fig. 4C).¹²⁷

564

565 **Epigenetic editing**

566 Beyond pharmacological inhibition, epigenetic editing has emerged as a precise strategy
567 for Xi reactivation. Song Lou et al conducted a genome-wide CRISPR/Cas9
568 loss-of-function screen in female mouse fibroblasts and identified several microRNAs
569 (miRNAs) as regulators of XCI, among which miR106a emerged as the most critical.
570 Inhibition of miR106a led to the reactivation of multiple genes on the Xi, including
571 *Mecp2*, glucose-6-phosphate dehydrogenase X-linked (*G6pdx*), lysosomal-associated

572 membrane protein 2 (*Lamp2*), and phosphoglycerate kinase 1 (*Pgk1*). Mechanistically,
573 miR106a exerts its function by directly binding to the Repeat A region of *Xist*, thereby
574 stabilizing *Xist* RNA and supporting its role in maintaining XCI. Inhibition of miR106a
575 also disrupts m⁶A modification and YTHDC1 binding, resulting in abnormal expression
576 and localization of *Xist*, thus impairing the balance of XCI. In a Rett syndrome mouse
577 model (*Tsix*^{ΔCpG-/+}; *Mecp2*^{+/-} females), delivery of a miR106a inhibitor, miR106a sponge
578 (miR106sp), via an adeno-associated virus serotype 9 (AAV9) vector significantly
579 increased *Mecp2* expression in the brain (restored to ~32% of wild-type levels) and
580 ameliorated multiple pathological phenotypes, including reduced lifespan, motor
581 coordination deficits, abnormal respiratory rhythms, and reduced brain volume (Fig.
582 4D).¹²⁸ This study highlights the role of miR106a in X chromosome inactivation, but the
583 exact mechanism by which it affects Xi transcription remains unclear. While miR106a is
584 thought to regulate *Xist* conformational changes and interactions, further research is
585 needed. This could potentially serve as a therapeutic approach for other X-linked
586 diseases.

587

588 A recent study employed dCas9-Tet1 (a DNA demethylation tool) and dCpf1-CTCF (a
589 chromatin insulator tool) to demethylate the *MECP2* promoter, successfully reactivating
590 Xi-linked *MECP2* in RTT human embryonic stem cells (hESCs). Notably, neurons
591 derived from methylation-edited RTT hESCs exhibited rescued cellular morphology and
592 electrophysiological deficits, demonstrating functional recovery.¹²⁹ Future studies are
593 needed to evaluate the effects of this epigenome editing approach in animal models of
594 RTT, particularly regarding its impact on behavioral outcomes.

595

596 In addition, reactivation of the silent wild-type *ALAS2* allele has been achieved in XLSA
597 by using Aza in mutated iPSC-derived hematopoietic progenitor cells.¹³⁰ In
598 neurodegeneration with brain iron accumulation, the normal WD Repeat domain 45
599 (*WDR45*) allele was activated in patient-derived fibroblasts through biotin
600 supplementation.¹³¹ Recent studies have also demonstrated that down-regulation of *Rnf12*
601 can reduce *Xist* levels,¹³² which may present a potential alternative approach for future
602 activation of Xi.

603

604 However, a major challenge in Xi reactivation is maintaining dosage balance to preserve
605 cellular homeostasis. For example, genetic ablation of *Ftx* in mice reduces *Xist* RNA
606 levels but leads to immune hyperactivation, predisposing animals to autoimmune
607 disorders.¹³³ Similarly, conditional deletion of *Xist* in murine hematopoietic
608 compartments induces aggressive myeloproliferative neoplasms and myelodysplastic
609 syndromes, underscoring the tumor-suppressive role of XCI in maintaining genomic
610 stability.¹³⁴

611

612 These findings illustrate the dual-edged nature of Xi reactivation strategies. While
613 restoring wild-type gene expression (*e.g.*, *MECP2*) may alleviate disease-specific deficits,
614 unintended off-target reactivation of other Xi-linked loci could lead to deleterious
615 consequences. For example, unsilenced oncogenes or immune regulators on the Xi might
616 promote malignancy or autoimmunity. Therefore, achieving locus-specific reactivation,
617 rather than global Xi derepression, is paramount to ensure therapeutic safety.

618

619 Over 20% of human X-linked genes can escape XCI, meaning they bypass the multiple
620 layers of epigenetic silencing established during XCI and maintain transcriptional activity
621 on the otherwise silent Xi. This results in biallelic expression from both X chromosomes
622 in females.^{135,136} *MECP2* is a facultative escape gene, meaning it is initially silenced
623 during development but can later be reactivated, demonstrating the potential for gene
624 reactivation. Additionally, constitutive escape genes have been identified, which are
625 expressed across most cell types, individuals, and developmental stages. These genes
626 seem to avoid XCI from the outset, showing little to no silencing during XCI.¹³⁷
627 Understanding the escape characteristics of different genes is therefore crucial for
628 developing effective strategies to treat X-linked diseases.

629

630 **Conclusions and perspectives**

631 Skewed XCI can result in the overexpression or silencing of pathogenic alleles,
632 significantly influencing disease severity. Recent studies have shown a strong correlation
633 between XCI skewing and various X-linked phenotypes, with over 80% of findings
634 linking disease severity to XCI skewness. However, diseases like RTT, Fabry disease,
635 and Duchenne muscular dystrophy, despite receiving substantial attention from
636 researchers, have yet to reach a unified conclusion. This is primarily due to differences in
637 the cohorts studied, including variations in age, mutation sites, and tissue types, as well as
638 inconsistencies in phenotypic assessment criteria, leading to considerable discrepancies in
639 the results. To reliably assess the impact of XCI skewing on phenotypic variability, future
640 studies should analyze familial cohorts with identical mutations, employ standardized

641 phenotyping, and integrate analyses of tissue specificity, age-related dynamics, and other
642 epigenetic modifiers.

643

644 Targeting *Xist* RNA to reactivate the inactive X chromosome has shown promising
645 improvements in disease severity in mouse models. Consequently, strategies aimed at
646 reactivating the Xi to restore wild-type gene expression have emerged as a potential
647 approach for treating X-linked diseases. Current therapeutic methods include XCIF
648 inhibitors (*e.g.*, targeting ACVR1/PDPK1), DNA methylation inhibitors (*e.g.*, Aza),
649 ASOs, JAK/STAT pathway inhibitors (*e.g.*, AG490), and epigenetic editing techniques
650 (*e.g.*, miR106a inhibition or dCas9-Tet1). However, each method carries its own
651 limitations, such as non-specific activation and safety concerns. In contrast, epigenetic
652 editing offers more precise targeting of regulatory elements, providing sustained and
653 efficient phenotypic rescue with superior locus specificity, which is crucial for
654 maintaining genomic dosage balance.

655

656 Furthermore, precise quantification of XCI skewing is critical for assessing disease risk
657 and evaluating therapeutic efficacy. Traditional DNA methylation detection methods,
658 owing to their technical maturity and operational simplicity, are widely used in initial
659 clinical screening and large-scale cohort studies. Compared with traditional methods,
660 XCI-ONT represents a future direction for more accurate determination of XCI skewness.
661 However, for potential clinical adoption, challenges such as cost reduction and
662 technology standardization need to be addressed.

663

664 Research into the mechanisms of XCI is essential for developing innovative therapeutic
665 strategies, with current efforts primarily concentrating on elucidating the role of the
666 *Xist/XIST*. In humans and mice, it is currently believed that *Xist/XIST* RNA recruits
667 chromatin modifiers and gene-silencing factors through its Repeat modules (*e.g.*, A, B, C,
668 D, E) to mediate chromatin remodeling and transcriptional repression on the Xi. However,
669 emerging evidence suggests that the mechanisms in humans differ from those in mice,
670 particularly in the initiation of XCI, the composition of *Xist* Repeat elements, and the
671 regulation by non-coding RNAs. A deeper understanding of the structural features and
672 regulatory mechanisms of *Xist/XIST* RNA in both mice and humans is essential for
673 advancing future therapeutic strategies.

674

675 **Conflict of interests**

676 The authors declared no conflict of interests.

677

678 **Funding**

679 This review was supported by the National Natural Science Foundation of China (No.
680 82471277) and the Natural Science Foundation of Hunan Province, China (No.
681 2024JJ5471).

682

683 **Acknowledgements**

684 The authors thank the funding sources for supporting this work.

685

686 **References**

- 687 1. Barr ML, Bertram EG. A morphological distinction between neurones of the male and
688 female, and the behaviour of the nucleolar satellite during accelerated nucleoprotein
689 synthesis. *Nature*. 1949;163(4148):676.
- 690 2. Ohno S, Hauschka TS. Allocycly of the X-chromosome in tumors and normal tissues.
691 *Cancer Res*. 1960;20:541-545.
- 692 3. Lyon MF. Gene action in the X-chromosome of the mouse (*Mus musculus* L.). *Nature*.
693 1961;190:372-373.
- 694 4. Lyon MF. X-chromosome inactivation as a system of gene dosage compensation to
695 regulate gene expression. *Prog Nucleic Acid Res Mol Biol*. 1989;36:119-130.
- 696 5. Brown CJ, Ballabio A, Rupert JL, et al. A gene from the region of the human X
697 inactivation centre is expressed exclusively from the inactive X chromosome. *Nature*.
698 1991;349(6304):38-44.
- 699 6. Viggiano E, Picillo E, Ergoli M, Cirillo A, Del Gaudio S, Politano L. Skewed
700 X-chromosome inactivation plays a crucial role in the onset of symptoms in carriers of
701 Becker muscular dystrophy. *J Gene Med*. 2017;19(4).
- 702 7. Brown CJ, Willard HF. The human X-inactivation centre is not required for
703 maintenance of X-chromosome inactivation. *Nature*. 1994;368(6467):154-156.
- 704 8. Zhang LF, Huynh KD, Lee JT. Perinucleolar targeting of the inactive X during S phase:
705 Evidence for a role in the maintenance of silencing. *Cell*. 2007;129(4):693-706.
- 706 9. Augui S, Nora EP, Heard E. Regulation of X-chromosome inactivation by the
707 X-inactivation centre. *Nat Rev Genet*. 2011;12(6):429-442.
- 708 10. Galupa R, Heard E. X-chromosome inactivation: A crossroads between chromosome
709 architecture and gene regulation. *Annu Rev Genet*. 2018;52:535-566.

- 710 11. Brown CJ, Hendrich BD, Rupert JL, et al. The human XIST gene: Analysis of a 17 kb
711 inactive X-specific RNA that contains conserved repeats and is highly localized within
712 the nucleus. *Cell*. 1992;71(3):527-542.
- 713 12. Brockdorff N, Ashworth A, Kay GF, et al. Conservation of position and exclusive
714 expression of mouse Xist from the inactive X chromosome. *Nature*.
715 1991;351(6324):329-331.
- 716 13. Okamoto I, Patrat C, Thépot D, et al. Eutherian mammals use diverse strategies to
717 initiate X-chromosome inactivation during development. *Nature*.
718 2011;472(7343):370-374.
- 719 14. Petropoulos S, Edsgård D, Reinius B, et al. Single-cell RNA-seq reveals lineage and
720 X chromosome dynamics in human preimplantation embryos. *Cell*.
721 2016;165(4):1012-1026.
- 722 15. Vallot C, Patrat C, Collier AJ, et al. XACT noncoding RNA competes with XIST in
723 the control of X chromosome activity during human early development. *Cell Stem Cell*.
724 2017;20(1):102-111.
- 725 16. Vallot C, Huret C, Lesecque Y, et al. XACT, a long noncoding transcript coating the
726 active X chromosome in human pluripotent cells. *Nat Genet*. 2013;45(3):239-241.
- 727 17. Alfeghaly C, Castel G, Cazottes E, et al. XIST dampens X chromosome activity in a
728 SPEN-dependent manner during early human development. *Nat Struct Mol Biol*.
729 2024;31(10):1589-1600.
- 730 18. Okamoto I, Arnaud D, Le Baccon P, et al. Evidence for *de novo* imprinted
731 X-chromosome inactivation independent of meiotic inactivation in mice. *Nature*.
732 2005;438(7066):369-373.

- 733 19. Okamoto I, Otte AP, Allis CD, Reinberg D, Heard E. Epigenetic dynamics of
734 imprinted X inactivation during early mouse development. *Science*.
735 2004;303(5658):644-649.
- 736 20. Mak W, Nesterova TB, de Napoles M, et al. Reactivation of the paternal X
737 chromosome in early mouse embryos. *Science*. 2004;303(5658):666-669.
- 738 21. Borensztein M, Okamoto I, Syx L, et al. Contribution of epigenetic landscapes and
739 transcription factors to X-chromosome reactivation in the inner cell mass. *Nat Commun*.
740 2017;8:1297.
- 741 22. Wutz A, Rasmussen TP, Jaenisch R. Chromosomal silencing and localization are
742 mediated by different domains of Xist RNA. *Nat Genet*. 2002;30(2):167-174.
- 743 23. Carter AC, Xu J, Nakamoto MY, et al. Spn links RNA-mediated endogenous
744 retrovirus silencing and X chromosome inactivation. *eLife*. 2020;9:e54508.
- 745 24. Dossin F, Pinheiro I, Żylicz JJ, et al. SPEN integrates transcriptional and epigenetic
746 control of X-inactivation. *Nature*. 2020;578(7795):455-460.
- 747 25. McHugh CA, Chen CK, Chow A, et al. The Xist lncRNA interacts directly with
748 SHARP to silence transcription through HDAC3. *Nature*. 2015;521(7551):232-236.
- 749 26. Jachowicz JW, Strehle M, Banerjee AK, Blanco MR, Thai J, Guttman M. Xist
750 spatially amplifies SHARP/SPEN recruitment to balance chromosome-wide silencing and
751 specificity to the X chromosome. *Nat Struct Mol Biol*. 2022;29(3):239-249.
- 752 27. Żylicz JJ, Bousard A, Žumer K, et al. The implication of early chromatin changes in
753 X chromosome inactivation. *Cell*. 2019;176(1-2):182-197.e23.

- 754 28. Coker H, Wei G, Moindrot B, Mohammed S, Nesterova T, Brockdorff N. The role of
755 the Xist 5' m⁶A region and RBM15 in X chromosome inactivation. *Wellcome Open Res.*
756 2020;5:31.
- 757 29. Patil DP, Chen CK, Pickering BF, et al. m⁶A RNA methylation promotes
758 XIST-mediated transcriptional repression. *Nature.* 2016;537(7620):369-373.
- 759 30. Lu Z, Guo JK, Wei Y, et al. Structural modularity of the XIST ribonucleoprotein
760 complex. *Nat Commun.* 2020;11(1):6163.
- 761 31. Bousard A, Raposo AC, Żylicz JJ, et al. The role of Xist-mediated polycomb
762 recruitment in the initiation of X-chromosome inactivation. *EMBO Rep.*
763 2019;20(10):e48019.
- 764 32. Pintacuda G, Wei G, Roustan C, et al. hnRNPk recruits PCGF3/5-PRC1 to the Xist
765 RNA B-repeat to establish polycomb-mediated chromosomal silencing. *Mol Cell.*
766 2017;68(5):955-969.e10.
- 767 33. Masui O, Corbel C, Nagao K, et al. Polycomb repressive complexes 1 and 2 are each
768 essential for maintenance of X inactivation in extra-embryonic lineages. *Nat Cell Biol.*
769 2023;25(1):134-144.
- 770 34. Nakamoto MY, Lammer NC, Batey RT, Wuttke DS. hnRNPk recognition of the B
771 motif of Xist and other biological RNAs. *Nucleic Acids Res.* 2020;48(16):9320-9335.
- 772 35. Colognori D, Sunwoo H, Kriz AJ, Wang CY, Lee JT. Xist deletion analysis reveals
773 an interdependency between Xist RNA and polycomb complexes for spreading along the
774 inactive X. *Mol Cell.* 2019;74(1):101-117.e10.

- 775 36. da Rocha ST, Boeva V, Escamilla-Del-Arenal M, et al. Jarid2 is implicated in the
776 initial Xist-induced targeting of PRC2 to the inactive X chromosome. *Mol Cell*.
777 2014;53(2):301-316.
- 778 37. Sunwoo H, Colognori D, Froberg JE, Jeon Y, Lee JT. Repeat E anchors Xist RNA to
779 the inactive X chromosomal compartment through CDKN1A-interacting protein (CIZ1).
780 *Proc Natl Acad Sci U S A*. 2017;114(40):10654-10659.
- 781 38. Ridings-Figueroa R, Stewart ER, Nesterova TB, et al. The nuclear matrix protein
782 CIZ1 facilitates localization of Xist RNA to the inactive X-chromosome territory. *Genes*
783 *Dev*. 2017;31(9):876-888.
- 784 39. Pandya-Jones A, Markaki Y, Serizay J, et al. A protein assembly mediates Xist
785 localization and gene silencing. *Nature*. 2020;587(7832):145-151.
- 786 40. Jeon Y, Lee JT. YY1 tethers Xist RNA to the inactive X nucleation center. *Cell*.
787 2011;146(1):119-133.
- 788 41. Chen CK, Blanco M, Jackson C, et al. Xist recruits the X chromosome to the nuclear
789 lamina to enable chromosome-wide silencing. *Science*. 2016;354(6311):468-472.
- 790 42. Yen ZC, Meyer IM, Karalic S, Brown CJ. A cross-species comparison of
791 X-chromosome inactivation in *Eutheria*. *Genomics*. 2007;90(4):453-463.
- 792 43. Lu Z, Zhang QC, Lee B, et al. RNA duplex map in living cells reveals higher-order
793 transcriptome structure. *Cell*. 2016;165(5):1267-1279.
- 794 44. Raposo AC, Casanova M, Gendrel AV, da Rocha ST. The tandem repeat modules of
795 Xist lncRNA: A Swiss army knife for the control of X-chromosome inactivation.
796 *Biochem Soc Trans*. 2021;49(6):2549-2560.

- 797 45. Chu C, Zhang QC, da Rocha ST, et al. Systematic discovery of Xist RNA binding
798 proteins. *Cell*. 2015;161(2):404-416.
- 799 46. Engreitz JM, Pandya-Jones A, McDonel P, et al. The Xist lncRNA exploits
800 three-dimensional genome architecture to spread across the X chromosome. *Science*.
801 2013;341(6147):1237973.
- 802 47. Costanzi C, Stein P, Worrada DM, Schultz RM, Pehrson JR. Histone macroH2A1 is
803 concentrated in the inactive X chromosome of female preimplantation mouse embryos.
804 *Development*. 2000;127(11):2283-2289.
- 805 48. Gendrel AV, Apedaile A, Coker H, et al. Smchd1-dependent and -independent
806 pathways determine developmental dynamics of CpG island methylation on the inactive
807 X chromosome. *Dev Cell*. 2012;23(2):265-279.
- 808 49. Escamilla-Del-Arenal M, da Rocha ST, Spruijt CG, et al. Cdy1, a new partner of the
809 inactive X chromosome and potential reader of H3K27me3 and H3K9me2. *Mol Cell Biol*.
810 2013;33(24):5005-5020.
- 811 50. Lee JT, Davidow LS, Warshawsky D. Tsix, a gene antisense to Xist at the
812 X-inactivation centre. *Nat Genet*. 1999;21(4):400-404.
- 813 51. van Bommel JG, Galupa R, Gard C, et al. The bipartite TAD organization of the
814 X-inactivation center ensures opposing developmental regulation of Tsix and Xist. *Nat*
815 *Genet*. 2019;51(6):1024-1034.
- 816 52. Dixon JR, Selvaraj S, Yue F, et al. Topological domains in mammalian genomes
817 identified by analysis of chromatin interactions. *Nature*. 2012;485(7398):376-380.

- 818 53. Gjaltema RAF, Schwämmle T, Kautz P, et al. Distal and proximal cis-regulatory
819 elements sense X chromosome dosage and developmental state at the Xist locus. *Mol*
820 *Cell*. 2022;82(1):190-208.e17.
- 821 54. Rosspopoff O, Cazottes E, Huret C, et al. Species-specific regulation of XIST by the
822 JPX/FTX orthologs. *Nucleic Acids Res*. 2023;51(5):2177-2194.
- 823 55. Nora EP, Lajoie BR, Schulz EG, et al. Spatial partitioning of the regulatory landscape
824 of the X-inactivation centre. *Nature*. 2012;485(7398):381-385.
- 825 56. Sun S, Del Rosario BC, Szanto A, Ogawa Y, Jeon Y, Lee JT. Jpx RNA activates Xist
826 by evicting CTCF. *Cell*. 2013;153(7):1537-1551.
- 827 57. Quesada-Espinosa JF, Garzón-Lorenzo L, Lezana-Rosales JM, et al. First female with
828 Allan-Herndon-Dudley syndrome and partial deletion of X-inactivation center.
829 *Neurogenetics*. 2021;22(4):343-346.
- 830 58. Jonkers I, Barakat TS, Achame EM, et al. RNF12 is an X-encoded dose-dependent
831 activator of X chromosome inactivation. *Cell*. 2009;139(5):999-1011.
- 832 59. Gontan C, Achame EM, Demmers J, et al. RNF12 initiates X-chromosome
833 inactivation by targeting REX1 for degradation. *Nature*. 2012;485(7398):386-390.
- 834 60. Barakat TS, Loos F, van Staveren S, et al. The trans-activator RNF12 and cis-acting
835 elements effectuate X chromosome inactivation independent of X-pairing. *Mol Cell*.
836 2014;53(6):965-978.
- 837 61. Makhlof M, Ouimette JF, Oldfield A, Navarro P, Neuillet D, Rougeulle C. A
838 prominent and conserved role for YY1 in Xist transcriptional activation. *Nat Commun*.
839 2014;5:4878.

- 840 62. Bowness JS, Almeida M, Nesterova TB, Brockdorff N. *YY1* binding is a
841 gene-intrinsic barrier to Xist-mediated gene silencing. *EMBO Rep.*
842 2024;25(5):2258-2277.
- 843 63. Furlan G, Gutierrez Hernandez N, Huret C, et al. The *ftx* noncoding locus controls X
844 chromosome inactivation independently of its RNA products. *Mol Cell.*
845 2018;70(3):462-472.e8.
- 846 64. Galupa R, Nora EP, Worsley-Hunt R, et al. A conserved noncoding locus regulates
847 random monoallelic Xist expression across a topological boundary. *Mol Cell.*
848 2020;77(2):352-367.e8.
- 849 65. Migeon BR, Chowdhury AK, Dunston JA, McIntosh I. Identification of *TSIX*,
850 encoding an RNA antisense to human *XIST*, reveals differences from its murine
851 counterpart: Implications for X inactivation. *Am J Hum Genet.* 2001;69(5):951-960.
- 852 66. Migeon BR, Lee CH, Chowdhury AK, Carpenter H. Species differences in *TSIX*/*Tsix*
853 reveal the roles of these genes in X-chromosome inactivation. *Am J Hum Genet.*
854 2002;71(2):286-293.
- 855 67. Monkhorst K, Jonkers I, Rentmeester E, Grosveld F, Gribnau J. X inactivation
856 counting and choice is a stochastic process: Evidence for involvement of an X-linked
857 activator. *Cell.* 2008;132(3):410-421.
- 858 68. Fieremans N, Van Esch H, Holvoet M, et al. Identification of intellectual disability
859 genes in female patients with a skewed X-inactivation pattern. *Hum Mutat.*
860 2016;37(8):804-811.

- 861 69. Plenge RM, Stevenson RA, Lubs HA, Schwartz CE, Willard HF. Skewed
862 X-chromosome inactivation is a common feature of X-linked mental retardation disorders.
863 *Am J Hum Genet.* 2002;71(1):168-173.
- 864 70. Nance WE. Genetic tests with a sex-linked marker: Glucose-6-phosphate
865 dehydrogenase. *Cold Spring Harb Symp Quant Biol.* 1964;29:415-425.
- 866 71. Viggiano E, Ergoli M, Picillo E, Politano L. Determining the role of skewed
867 X-chromosome inactivation in developing muscle symptoms in carriers of Duchenne
868 muscular dystrophy. *Hum Genet.* 2016;135(7):685-698.
- 869 72. Eble TN, Sutton VR, Sangi-Haghpeykar H, et al. Non-random X chromosome
870 inactivation in Aicardi syndrome. *Hum Genet.* 2009;125(2):211-216.
- 871 73. Wang X, Reid Sutton V, Omar Peraza-Llanes J, et al. Mutations in X-linked PORCN,
872 a putative regulator of Wnt signaling, cause focal dermal hypoplasia. *Nat Genet.*
873 2007;39(7):836-838.
- 874 74. Badens C, Martini N, Courrier S, et al. ATRX syndrome in a girl with a heterozygous
875 mutation in the ATRX Zn finger domain and a totally skewed X-inactivation pattern. *Am*
876 *J Med Genet A.* 2006;140(20):2212-2215.
- 877 75. Cañueto J, Girós M, Ciria S, et al. Clinical, molecular and biochemical
878 characterization of nine Spanish families with Conradi-Hünemann-Happle syndrome:
879 New insights into X-linked dominant chondrodysplasia punctata with a comprehensive
880 review of the literature. *Br J Dermatol.* 2012;166(4):830-838.
- 881 76. Michaud V, Defoort-Dhellemmes S, Drumare I, et al. Clinical and molecular findings
882 of FRMD7 related congenital nystagmus as a differential diagnosis of ocular albinism.
883 *Ophthalmic Genet.* 2019;40(2):161-164.

- 884 77. Xu J, Khincha PP, Giri N, Alter BP, Savage SA, Wong JMY. Investigation of
885 chromosome X inactivation and clinical phenotypes in female carriers of DKC1
886 mutations. *Am J Hematol*. 2016;91(12):1215-1220.
- 887 78. Viggiano E, Picillo E, Cirillo A, Politano L. Comparison of X-chromosome
888 inactivation in Duchenne muscle/myocardium-manifesting carriers, non-manifesting
889 carriers and related daughters. *Clin Genet*. 2013;84(3):265-270.
- 890 79. Echevarria L, Benistan K, Toussaint A, et al. X-chromosome inactivation in female
891 patients with Fabry disease. *Clin Genet*. 2016;89(1):44-54.
- 892 80. Juchniewicz P, Kloska A, Tylki-Szymańska A, et al. Female Fabry disease patients
893 and X-chromosome inactivation. *Gene*. 2018;641:259-264.
- 894 81. Alvarez-Mora MI, Rodriguez-Revilla L, Feliu A, Badenas C, Madrigal I, Milà M.
895 Skewed X inactivation in women carrying the FMR1 premutation and its relation with
896 fragile-X-associated tremor/ataxia syndrome. *Neurodegener Dis*. 2016;16(3-4):290-292.
- 897 82. Garagiola I, Mortarino M, Siboni SM, et al. X Chromosome inactivation: A modifier
898 of factor VIII and IX plasma levels and bleeding phenotype in Haemophilia carriers. *Eur*
899 *J Hum Genet*. 2021;29(2):241-249.
- 900 83. Okumura K, Fujimori Y, Takagi A, et al. Skewed X chromosome inactivation in
901 fraternal female twins results in moderately severe and mild haemophilia B. *Haemophilia*.
902 2008;14(5):1088-1093.
- 903 84. Torres RJ, Puig JG. Skewed X inactivation in Lesch-Nyhan disease carrier females. *J*
904 *Hum Genet*. 2017;62(12):1079-1083.

- 905 85. Cau M, Addis M, Congiu R, et al. A locus for familial skewed X chromosome
906 inactivation maps to chromosome Xq25 in a family with a female manifesting Lowe
907 syndrome. *J Hum Genet.* 2006;51(11):1030-1036.
- 908 86. Sirleto P, Surace C, Santos H, et al. Lyonization effects of the t(X;16) translocation
909 on the phenotypic expression in a rare female with Menkes disease. *Pediatr Res.*
910 2009;65(3):347-351.
- 911 87. Desai V, Donsante A, Swoboda KJ, Martensen M, Thompson J, Kaler SG. Favorably
912 skewed X-inactivation accounts for neurological sparing in female carriers of Menkes
913 disease. *Clin Genet.* 2011;79(2):176-182.
- 914 88. van Rahden VA, Fernandez-Vizarra E, Alawi M, et al. Mutations in NDUFB11,
915 encoding a complex I component of the mitochondrial respiratory chain, cause
916 microphthalmia with linear skin defects syndrome. *Am J Hum Genet.*
917 2015;96(4):640-650.
- 918 89. Piña-Aguilar RE, Zaragoza-Arévalo GR, Rau I, et al. Mucopolysaccharidosis type II
919 in a female carrying a heterozygous stop mutation of the iduronate-2-sulfatase gene and
920 showing a skewed X chromosome inactivation. *Eur J Med Genet.* 2013;56(3):159-162.
- 921 90. Scala M, Traverso M, Capra V, et al. Pelizaeus-Merzbacher disease due to PLP1
922 frameshift mutation in a female with nonrandom skewed X-chromosome inactivation.
923 *Neuropediatrics.* 2019;50(4):268-270.
- 924 91. Horga A, Woodward CE, Mills A, et al. Differential phenotypic expression of a novel
925 PDHA1 mutation in a female monozygotic twin pair. *Hum Genet.*
926 2019;138(11-12):1313-1322.

- 927 92. Yano S, Baskin B, Bagheri A, et al. Familial Simpson-Golabi-Behmel syndrome:
928 Studies of X-chromosome inactivation and clinical phenotypes in two female individuals
929 with GPC3 mutations. *Clin Genet*. 2011;80(5):466-471.
- 930 93. Wang Z, Yan A, Lin Y, Xie H, Zhou C, Lan F. Familial skewed X chromosome
931 inactivation in adrenoleukodystrophy manifesting heterozygotes from a Chinese pedigree.
932 *PLoS One*. 2013;8(3):e57977.
- 933 94. Shimizu Y, Nagata M, Usui J, et al. Tissue-specific distribution of an alternatively
934 spliced COL4A5 isoform and non-random X chromosome inactivation reflect phenotypic
935 variation in heterozygous X-linked Alport syndrome. *Nephrol Dial Transplant*.
936 2006;21(6):1582-1587.
- 937 95. Suzuki R, Sakakibara N, Murakami S, et al. Genotype and X-chromosome
938 inactivation are associated with disease severity in females with X-linked Alport
939 syndrome. *Nephrol Dial Transplant*. 2025;40(4):688-695.
- 940 96. López-Hernández I, Deswarte C, Alcantara-Ortigoza MÁ, et al. Skewed
941 X-inactivation in a female carrier with X-linked chronic granulomatous disease. *Iran J*
942 *Allergy Asthma Immunol*. 2019;18(4):447-451.
- 943 97. Pavlovsky M, Fuchs-Telem D, Nousbeck J, Sarig O, Sprecher E. Molecular evidence
944 for the role of X-chromosome inactivation in linear presentation of X-linked hypohidrotic
945 ectodermal dysplasia. *Clin Exp Dermatol*. 2012;37(2):186-188.
- 946 98. Brancaleoni V, Balwani M, Granata F, et al. X-chromosomal inactivation directly
947 influences the phenotypic manifestation of X-linked protoporphyria. *Clin Genet*.
948 2016;89(1):20-26.

- 949 99. Aivado M, Gattermann N, Rong A, et al. X-linked sideroblastic anemia associated
950 with a novel ALAS2 mutation and unfortunate skewed X-chromosome inactivation
951 patterns. *Blood Cells Mol Dis.* 2006;37(1):40-45.
- 952 100. Amir RE, Van den Veyver IB, Wan M, Tran CQ, Francke U, Zoghbi HY. Rett
953 syndrome is caused by mutations in X-linked MECP2, encoding methyl-CpG-binding
954 protein 2. *Nat Genet.* 1999;23(2):185-188.
- 955 101. Chahrour M, Zoghbi HY. The story of Rett syndrome: From clinic to neurobiology.
956 *Neuron.* 2007;56(3):422-437.
- 957 102. Girard M, Couvert P, Carrié A, et al. Parental origin of *de novo* MECP2 mutations
958 in Rett syndrome. *Eur J Hum Genet.* 2001;9(3):231-236.
- 959 103. Trappe R, Laccone F, Cobilanschi J, et al. MECP2 mutations in sporadic cases of
960 Rett syndrome are almost exclusively of paternal origin. *Am J Hum Genet.*
961 2001;68(5):1093-1101.
- 962 104. Zhu X, Li M, Pan H, Bao X, Zhang J, Wu X. Analysis of the parental origin of *de*
963 *novo* MECP2 mutations and X chromosome inactivation in 24 sporadic patients with Rett
964 syndrome in China. *J Child Neurol.* 2010;25(7):842-848.
- 965 105. Knudsen GPS, Neilson TCS, Pedersen J, et al. Increased skewing of X chromosome
966 inactivation in Rett syndrome patients and their mothers. *Eur J Hum Genet.*
967 2006;14(11):1189-1194.
- 968 106. Wan M, Lee SS, Zhang X, et al. Rett syndrome and beyond: Recurrent spontaneous
969 and familial MECP2 mutations at CpG hotspots. *Am J Hum Genet.*
970 1999;65(6):1520-1529.

- 971 107. Huppke P, Maier EM, Warnke A, Brendel C, Laccone F, Gärtner J. Very mild cases
972 of Rett syndrome with skewed X inactivation. *J Med Genet.* 2006;43(10):814-816.
- 973 108. Villard L, Kpebe A, Cardoso C, Chelly PJ, Tardieu PM, Fontes M. Two affected
974 boys in a Rett syndrome family: Clinical and molecular findings. *Neurology.*
975 2000;55(8):1188-1193.
- 976 109. Archer H, Evans J, Leonard H, et al. Correlation between clinical severity in patients
977 with Rett syndrome with a p.R168X or p.T158M MECP2 mutation, and the direction and
978 degree of skewing of X-chromosome inactivation. *J Med Genet.* 2007;44(2):148-152.
- 979 110. Fang X, Butler KM, Abidi F, et al. Analysis of X-inactivation status in a Rett
980 syndrome natural history study cohort. *Mol Genet Genomic Med.* 2022;10(5):e1917.
- 981 111. Riguzzi P, Sabbatini D, Fusto A, et al. Deep characterization of females with
982 heterozygous Duchenne muscular dystrophy mutations. *J Neurol.* 2025;272(3):244.
- 983 112. Viggiano E, Politano L. X chromosome inactivation in carriers of Fabry disease:
984 Review and meta-analysis. *Int J Mol Sci.* 2021;22(14):7663.
- 985 113. Bittel DC, Theodoro MF, Kibiryeva N, Fischer W, Talebizadeh Z, Butler MG.
986 Comparison of X-chromosome inactivation patterns in multiple tissues from human
987 females. *J Med Genet.* 2008;45(5):309-313.
- 988 114. Sharp AJ, Stathaki E, Migliavacca E, et al. DNA methylation profiles of human
989 active and inactive X chromosomes. *Genome Res.* 2011;21(10):1592-1600.
- 990 115. Keith DH, Singer-Sam J, Riggs AD. Active X chromosome DNA is unmethylated at
991 eight CCGG sites clustered in a guanine-plus-cytosine-rich island at the 5' end of the
992 gene for phosphoglycerate kinase. *Mol Cell Biol.* 1986;6(11):4122-4125.

- 993 116. Allen RC, Zoghbi HY, Moseley AB, Rosenblatt HM, Belmont JW. Methylation of
994 HpaII and HhaI sites near the polymorphic CAG repeat in the human androgen-receptor
995 gene correlates with X chromosome inactivation. *Am J Hum Genet.*
996 1992;51(6):1229-1239.
- 997 117. Machado FB, Machado FB, Faria MA, et al. 5meCpG epigenetic marks neighboring
998 a primate-conserved core promoter short tandem repeat indicate X-chromosome
999 inactivation. *PLoS One.* 2014;9(7):e103714.
- 1000 118. Johansson J, Lidéus S, Höijer I, et al. A novel quantitative targeted analysis of
1001 X-chromosome inactivation (XCI) using nanopore sequencing. *Sci Rep.*
1002 2023;13(1):12856.
- 1003 119. Vacca M, Della Ragione F, Scalabrì F, D'Esposito M. X inactivation and
1004 reactivation in X-linked diseases. *Semin Cell Dev Biol.* 2016;56:78-87.
- 1005 120. Kubota T, Nonoyama S, Tonoki H, et al. A new assay for the analysis of
1006 X-chromosome inactivation based on methylation-specific PCR. *Hum Genet.*
1007 1999;104(1):49-55.
- 1008 121. Rupert JL, Brown CJ, Willard HF. Direct detection of non-random X chromosome
1009 inactivation by use of a transcribed polymorphism in the XIST gene. *Eur J Hum Genet.*
1010 1995;3(6):333-343.
- 1011 122. Mortazavi A, Williams BA, McCue K, Schaeffer L, Wold B. Mapping and
1012 quantifying mammalian transcriptomes by RNA-Seq. *Nat Methods.* 2008;5(7):621-628.
- 1013 123. Guy J, Gan J, Selfridge J, Cobb S, Bird A. Reversal of neurological defects in a
1014 mouse model of Rett syndrome. *Science.* 2007;315(5815):1143-1147.

- 1015 124. Bhatnagar S, Zhu X, Ou J, et al. Genetic and pharmacological reactivation of the
1016 mammalian inactive X chromosome. *Proc Natl Acad Sci U S A*.
1017 2014;111(35):12591-12598.
- 1018 125. Przanowski P, Wasko U, Zheng Z, et al. Pharmacological reactivation of inactive
1019 X-linked Mecp2 in cerebral cortical neurons of living mice. *Proc Natl Acad Sci U S A*.
1020 2018;115(31):7991-7996.
- 1021 126. Carrette LLG, Wang CY, Wei C, et al. A mixed modality approach towards Xi
1022 reactivation for Rett syndrome and other X-linked disorders. *Proc Natl Acad Sci U S A*.
1023 2018;115(4):E668-E675.
- 1024 127. Lee HM, Kuijjer MB, Ruiz Blanes N, et al. A small-molecule screen reveals novel
1025 modulators of MeCP2 and X-chromosome inactivation maintenance. *J Neurodev Disord*.
1026 2020;12(1):29.
- 1027 128. Lou S, DJiaka Tihagam R, Wasko UN, et al. Targeting microRNA-dependent
1028 control of X chromosome inactivation improves the Rett syndrome phenotype. *Nat*
1029 *Commun*. 2025;16(1):6169.
- 1030 129. Qian J, Guan X, Xie B, et al. Multiplex epigenome editing of MECP2 to rescue Rett
1031 syndrome neurons. *Sci Transl Med*. 2023;15(679):eadd4666.
- 1032 130. Morimoto Y, Chonabayashi K, Kawabata H, et al. Azacitidine is a potential
1033 therapeutic drug for pyridoxine-refractory female X-linked sideroblastic anemia. *Blood*
1034 *Adv*. 2022;6(4):1100-1114.
- 1035 131. Reche-López D, Romero-González A, Álvarez-Córdoba M, et al. Biotin induces
1036 inactive chromosome X reactivation and corrects physiopathological alterations in
1037 beta-propeller-protein-associated neurodegeneration. *Int J Mol Sci*. 2025;26(3):1315.

- 1038 132. Sripathy S, Leko V, Adrianse RL, et al. Screen for reactivation of MeCP2 on the
1039 inactive X chromosome identifies the BMP/TGF- β superfamily as a regulator of XIST
1040 expression. *Proc Natl Acad Sci U S A*. 2017;114(7):1619-1624.
- 1041 133. Huret C, Ferrayé L, David A, et al. Altered X-chromosome inactivation predisposes
1042 to autoimmunity. *Sci Adv*. 2024;10(18):eadn6537.
- 1043 134. Yildirim E, Kirby JE, Brown DE, et al. Xist RNA is a potent suppressor of
1044 hematologic cancer in mice. *Cell*. 2013;152(4):727-742.
- 1045 135. Carrel L, Willard HF. X-inactivation profile reveals extensive variability in X-linked
1046 gene expression in females. *Nature*. 2005;434(7031):400-404.
- 1047 136. Balaton BP, Brown CJ. Escape artists of the X chromosome. *Trends Genet*.
1048 2016;32(6):348-359.
- 1049 137. Patrat C, Okamoto I, Diabangouaya P, et al. Dynamic changes in paternal
1050 X-chromosome activity during imprinted X-chromosome inactivation in mice. *Proc Natl*
1051 *Acad Sci U S A*. 2009;106(13):5198-5203.
- 1052

Table 1 Association of X chromosome inactivation (XCI) skewing and phenotypes in X-linked disorders.

X-linked disease	OMIM	Gene	Study population	Detection method	Phenotype and X-inactivation correlation	Reference
Aicardi syndrome	304050	<i>Xp22</i>	35 females	HUMARA assay	Non-random XCI is associated with a high neurological composite severity score	72
Angioma serpiginosum	300652	<i>PORCN</i>	A three-generation family	HUMARA assay	Variability in severity is explained by functional mosaicism in females because of XCI	73
ATRX syndrome	301040	<i>ATRX</i>	A 4-year-old girl	The methylation patterns at the <i>AR</i> and at the <i>FMRI</i> loci	The active chromosome carries a heterozygous mutation in the <i>ATRX</i> gene	74
Becker muscular dystrophy	300376	<i>DMD</i>	36 carriers from 11 families	HUMARA assay	The onset of symptoms in the carriers is related to a skewed XCI	6

Conradi-Hünemann-Happle syndrome	302960	<i>EBP</i>	13 female patients belonging to 9 Spanish families	HUMARA assay	The skewed X chromosome inactivation may explain the clinical phenotype in some familial cases	75
Congenital nystagmus	310700	<i>FRMD7</i>	A four-generation family with 5 affected members	HUMARA assay	The presence of the disease in one affected girl is due to the preferential activation of the X chromosome bearing the pathogenic variant	76
Dyskeratosis congenita	305000	<i>DKC1</i>	7 subjects in 5 families	HUMARA assay	All female carriers had similarly skewed X-inactivation in multiple tissue types, regardless of phenotype	77
Duchenne muscular dystrophy	310200	<i>DMD</i>	54 patients	HUMARA assay	Clinical manifestations in carriers are associated with non-random patterns of XCI	78
Fabry disease	301500	<i>GLA</i>	56 consecutive female patients	HUMARA assay	Skewed XCI in female patients affects the disease course based on the	79

					predominantly expressed allele	
			12 female patients		XCI is not a main factor in the phenotype variability of Fabry disease manifestation in heterozygous females	80
Fragile-X-associated tremor/ataxia syndrome	300623	<i>FMRI</i>	10 women patients and 21 without disease	<i>FMRI</i> CGG repeats and methylation status and HUMARA assay	The skewed XCI of the normal FMR1 allele may be a risk factor for the development of this disease	81
Hemophilia A	306700	<i>F8</i>	215 carriers	HUMARA assay	Skewed XCI may contribute to the low expression of clotting factor levels and bleeding symptoms	82
Hemophilia B	306900	<i>F9</i>	Twin girls	Polymorphic markers, SNP	Skewed inactivation causes severe and mild phenotypes	83

Hypoxanthine-guanine phosphoribosyltransferase deficiency	308000	<i>HPRT1</i>	109 women belonging to 31 families	HUMARA assay	There is a correlation between skewed XCI and the severity of the phenotype	84
Lowe syndrome	300179	<i>OCRL</i>	12 subjects belonging to a large four-generation family	HUMARA assay	Lowe syndrome may manifest the full phenotype in females because of the skewed X inactivation	85
Menkes disease	309400	<i>ATP7A</i>	A 6.5-month-old girl 10 members of a family	HUMARA assay	The patient showed a severe phenotype because of the inactivation of the normal X chromosome in all the cells All six female heterozygotes show skewed X-inactivation, with preferential silencing of the mutant X chromosome	86 87
Microphthalmia with linear skin defects	309801	<i>HCCS</i>	11 females	HUMARA assay	The degree of skewed X-inactivation causes clinical variability	88

Mucopolysaccharidosis type II	309900	<i>IDS</i>	The second child of healthy, non-consanguineous parents	HUMARA assay	A skewed inactivation silencing preferentially the X chromosome carrying the wild-type IDS gene should be responsible for the disease manifestation	89
Pelizaeus-Merzbacher disease	312080	<i>PLP1</i>	A girl with healthy parents and 2 elder brothers	HUMARA assay	The patient is severely symptomatic due to the unfavorable X-inactivation pattern	90
Pyruvate dehydrogenase complex deficiency	312170	<i>PDHA1</i>	A female monozygotic twin pair	HUMARA assay	X-chromosome inactivation may influence the phenotypic expression of the same mutation in heterozygous females	91
Simpson-Golabi-Behmel syndrome type 1	312870	<i>GPC3</i>	3 siblings	HUMARA assay and the analysis of the CCG repeats of	These X-inactivation studies with peripheral blood DNA specimens can provide explanations for the phenotypic	92

				the Fragile XE (<i>FRAXE</i>) gene	features in the two female subjects	
X-linked adrenoleukodystrophy	300100	<i>ABCD1</i>	5 heterozygous females	HUMARA assay	Skewed XCI in favor of the mutant ABCD1 allele would be associated with the manifestation of heterozygous symptoms	93
X-linked Alport syndrome	303630	<i>COL4A5</i>	A 23-year-old female and her mother 74 adult female patients	HUMARA assay	Non-random X-chromosome inactivation with a normal allele affects the phenotype of heterozygous individuals Genotype and XCI are factors associated with severity in females with this disease	94 95
X-linked chronic granulomatous disease	306400	<i>CYBB</i>	The female witness and her one son and one daughter	HUMARA assay	Skewed X-inactivation causes disease in carriers	96

X-linked hypohidrotic ectodermal dysplasia	305100	<i>EDA</i>	The female witness and her son	RT-PCR	XCI explained patches of abnormal skin	97
X-linked protoporphyria	300752	<i>ALAS2</i>	11 heterozygous females	HUMARA assay and ZMYM type 3 short tandem repeat polymorphisms	The Xi pattern directly influences the penetrance and the severity of the phenotype in heterozygous females	98
X-linked sideroblastic anemia	300751	<i>ALAS2</i>	3 women from a family	HUMARA assay	Their differing clinical courses can be explained by the X-inactivation patterns of granulocytes and bone marrow cells	99

Note: HUMARA, human androgen receptor; SNP, single-nucleotide polymorphism; *FMR1*, fragile X messenger ribonucleoprotein 1.

Table 2 Comparative overview of X chromosome inactivation (XCI) detection methods: Core features and trade-offs.

Method	Target	Principle	Advantages	Limitations
HUMARA assay	DNA methylation (<i>AR</i> gene)	PCR, methylation-sensitive enzymatic digestion (HpaII), and fragment length analysis	Widely used; high heterozygosity (CAG repeats)	PCR artifacts; fluorescence detection bias; enzyme digestion efficiency dependence
Dual <i>AR/FP2</i> approach	DNA methylation (<i>AR</i> gene and <i>FP2</i> gene)	Combines <i>AR</i> and <i>FP2</i> analysis to improve reliability	Reduces single-locus bias; higher reliability	Increased technical complexity; still PCR-dependent
Bisulfite sequencing	DNA methylation (genome-wide)	Bisulfite converts C to U (unmethylated); methylation-specific sequencing	No enzymes; quantitative	Conversion inefficiency; complex design
XCI-ONT	DNA methylation and	CRISPR-enriched loci,	No PCR bias;	Expensive; requires a

	repeat length	nanopore sequencing (direct methylation and repeat analysis)	high-resolution data	nanopore platform
RNA sequencing and SNP analysis	RNA expression (allele-specific)	RNA sequencing; SNP arrays	Direct transcription insight; tissue-specific	Needs high-quality RNA; No methylation data

Note: HUMARA, human androgen receptor; *AR*, androgen receptor; *RP2*, retinitis pigmentosa 2; SNP, single-nucleotide polymorphism; HpaII, haemophilus parainfluenzae II; ONT, Oxford Nanopore Technologies.

Figure legends

Figure 1 Key regulatory genes and elements in X chromosome inactivation (XCI). **(A)** Differences in the initiation of XCI between mice and humans. In humans, both X chromosomes undergo transcriptional dampening during the early pre-implantation stage, with X-inactive specific transcript (*XIST*) expressed from both X chromosomes to ensure dosage compensation. *XACT* transiently co-expresses with *XIST*, but does not regulate *XIST* or X-linked gene expression. In mice, imprinted XCI (iXCI) silences the paternal X chromosome (Xp) early, beginning at the 4-cell stage. During the late blastocyst stage, Xp is reactivated in the inner cell mass (ICM). Random X-chromosome inactivation (rXCI) occurs at the late blastocyst stage in both mice and humans. **(B)** Functional domains of *Xist* RNA and late epigenetic changes. Repeat A initiates transcriptional silencing by interacting with the SPlit ENds (SPEN) protein, which further recruits chromatin-modifying complexes to promote histone H3/H4 deacetylation. It also recruits repressor complexes, including nuclear receptor corepressor (NCoR), silencing mediator of retinoic acid and thyroid hormone receptor (SMRT), and nucleosome remodeling deacetylase (NuRD), to the inactive X chromosome (Xi), facilitating histone deacetylation via histone deacetylase 3 (HDAC3). Additionally, repeat A recruits SPOC-containing proteins, such as RNA-binding motif proteins 15 (RBM15) and 15B (RBM15B), which mediate gene silencing through N6-methyladenosine (m⁶A) RNA methylation. m⁶A modifications in the *Xist* repeat A region are recognized by the m⁶A reader YTH domain containing 1 (YTHDC1), contributing to transcriptional silencing. Repeats B and C maintain Xi in its inactive state by recruiting polycomb repressive complexes 1 (PRC1) and 2 (PRC2). PRC1 mediates

the silencing of CpG island (CGI)-associated genes through histone H2A lysine 119 mono-ubiquitination (H2AK119ub1), while PRC2 targets a distinct or partially overlapping set of genes via histone H3 lysine 27 trimethylation (H3K27me3). HNRNPK recruits the PCGF3/5-PRC1 complex, which catalyzes H2A lysine 119 ubiquitination (H2AK119ub), marking silenced chromatin regions. Jarid2, a cofactor of PRC2, recognizes H2AK119ub and promotes PRC2 recruitment to the Xi, further reinforcing heterochromatin formation. The Repeat E module anchors *Xist* RNA to the Xi, crucial for maintaining XCI. CDKN1A-interacting zinc finger protein 1 (CIZ1) aids *Xist*'s association with the nuclear matrix in a cell lineage-specific manner. Four proteins, PTBP1, MATR3, TDP-43, and CELF1, interact with Repeat E, forming a CIZ1-independent complex that stabilizes *Xist* RNA after transcriptional silencing by Repeat A and PcG recruitment via Repeat B/C. The roles of Repeats D and F are less well defined, though Repeat F may influence *Xist* RNA stability. Late-stage epigenetic modifications include macroH2A enrichment on the Xi, DNA methylation of CpG islands by DNA (cytosine-5)-methyltransferase 3B (DNMT3B), and histone H3 lysine 9 dimethylation (H3K9me2). H3K9me2 recruits the chromodomain Y-like (CDYL)-G9A-MAX gene-associated (MGA) complex, which may propagate H3K9me2 across the Xi.

(C) Regulatory landscape of the X inactivation center (XIC). The XIC orchestrates XCI, with the *Xist* gene acting as the central regulator. *Xist* expression is negatively controlled by the antisense transcript X-inactive specific transcript antisense (*Tsix*), which overlaps *Xist* and is transcribed in the opposite direction. *Tsix* is located within the *Tsix* topologically associating domain (TAD), while *Xist* resides in the adjacent *Xist* TAD. The *Xist* TAD contains several positive regulators of *Xist*, including the

non-coding RNAs *Jpx* and *Ftx*, the RING finger protein 12 gene (*Rnf12*), and the enhancer-associated transcript *Xert*. *Linx*, a long non-coding RNA, acts as a distal cis-repressor of *Xist*, and the *Xite* enhancer drives *Tsix* transcription. *Jpx* RNA activates *Xist* by displacing CCCTC-binding factor (CTCF), an RNA-binding protein that represses *Xist* transcription. During differentiation, the degradation of the pluripotency factor REX1 (also known as zinc finger protein 42, ZFP42) relieves repression of *Xist*, enabling its upregulation. Additionally, the transcription factor Yin-Yang 1 (YY1) competes with REX1 for binding to the *Xist* 5' region, thereby activating the *Xist* promoter. Xa, active X chromosome; Xi, inactive X chromosome; Xp, paternal X chromosome; Xm, maternal X chromosome.

Figure 2 Impact of X chromosome inactivation (XCI) skewing on disease phenotype.

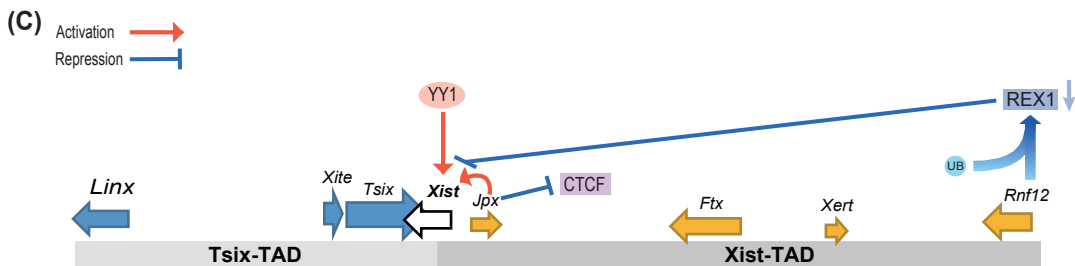
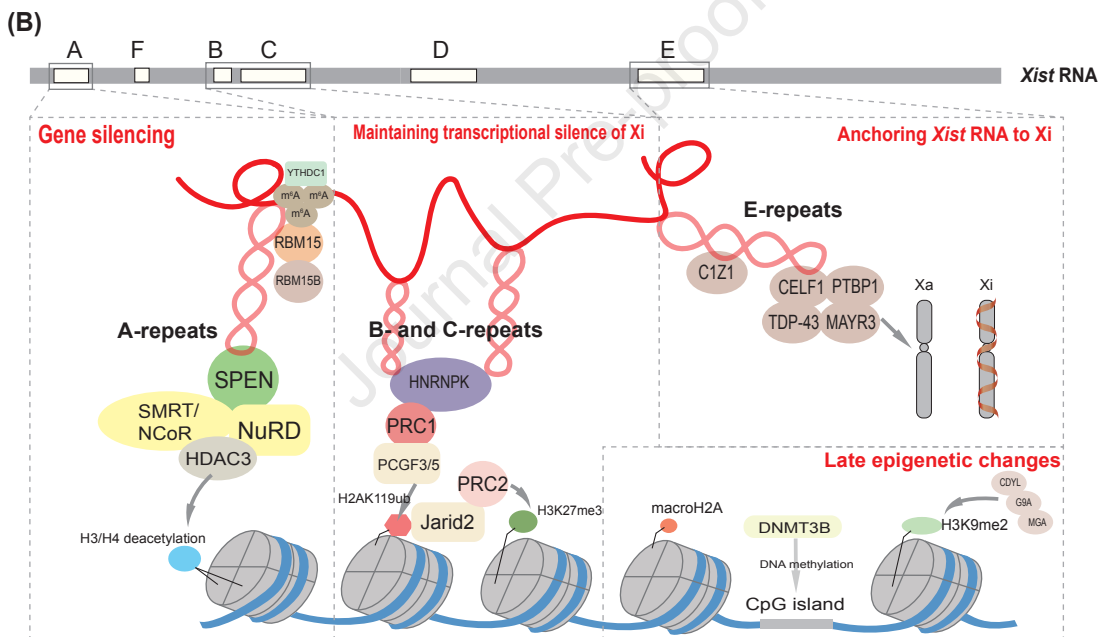
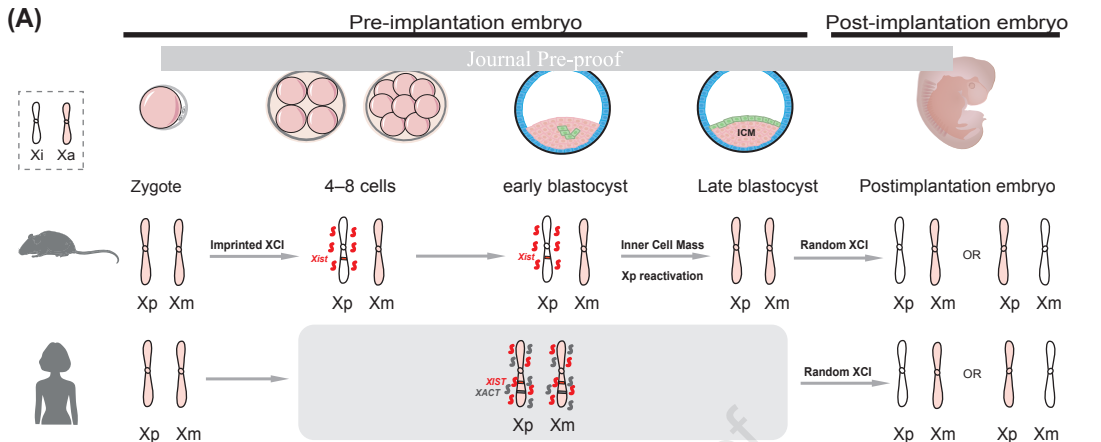
Under random XCI (WT:Mut = 50:50), cells exhibit an equal expression of both wild-type and mutant alleles, leading to an asymptomatic phenotype. In non-random XCI, the degree of skewing towards the mutant allele directly correlates with the increasing severity of clinical manifestations. At WT:Mut = 80:20, the preferential inactivation of the mutant allele results in mild clinical symptoms. At WT:Mut = 20:80, inactivation of the wild-type allele predominates, leading to severe functional deficits. At WT:Mut = 0:100, complete inactivation of the wild-type allele causes profound disability and life-threatening complications. Conversely, when XCI is fully skewed towards the wild-type allele (WT:Mut = 100:0), inactivation of the mutant allele restores wild-type expression, resulting in a phenotypically normal outcome. WT:Mut: X-inactivation ratio (Wild-type to Mutant).

Figure 3 Detection methods for X chromosome inactivation (XCI) ratios. **(A)**

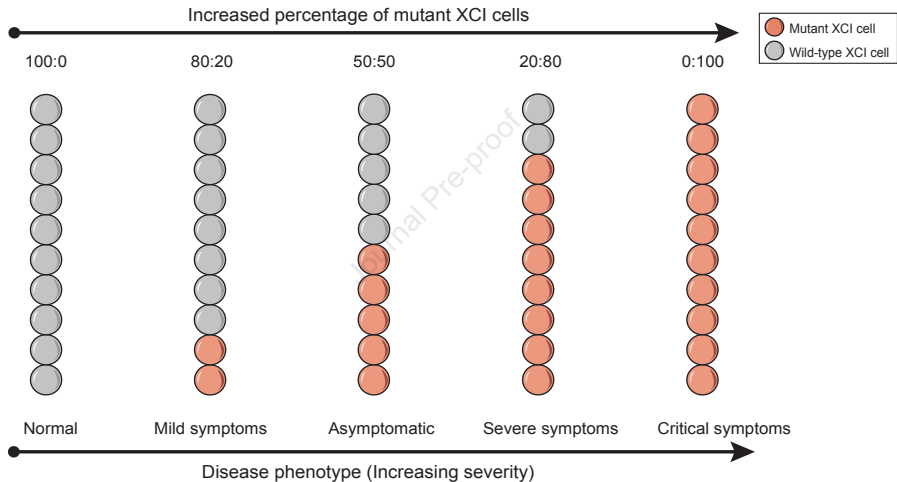
Methylation-sensitive restriction enzyme analysis of XCI ratio using haemophilus parainfluenzae II (HpaII). The methylation-sensitive restriction enzyme HpaII was utilized to target the CAG_n repeat site in the *AR* gene and the GAAA_n repeat site in the *RP2* gene on the X chromosome. Parental alleles, distinguished by varying repeat copy numbers, were differentiated through fragment length analysis of PCR-amplified repeat sequences. The PCR products were subsequently analyzed using capillary electrophoresis with fluorescence detection, and the XCI ratio was determined based on the peak area ratio. **(B)** CRISPR-Cas9-based XCI detection with Oxford Nanopore Technologies (ONT) sequencing. The XCI-ONT method uses CRISPR-Cas9 to cut the DNA on both sides of a ~3 kb region of interest (ROI), which spans 116 CpG sites in *AR* and 58 CpG sites in *RP2*. The region is then subjected to DNA sequencing, with methylation detection performed simultaneously using ONT sequencing technology. The XCI status is calculated based on the average methylation frequency of the region, followed by the calculation of the average methylation ratio between alleles for each gene. **(C)** RNA-sequencing-based XCI ratio estimation using heterozygous single-nucleotide polymorphisms (SNPs). After performing RNA-sequencing analysis on patient samples, the resulting sequence reads are aligned with the reference genome to identify heterozygous X-linked SNPs. The expression ratios of the paternal and maternal alleles at these SNP sites are then used to estimate the average XCI ratio. X_a, active X chromosome; X_i, inactive X chromosome; P, paternal allele; M, maternal allele.

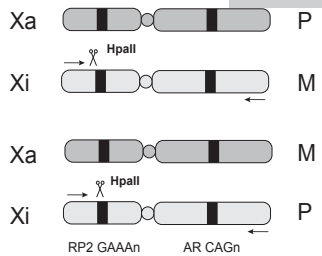
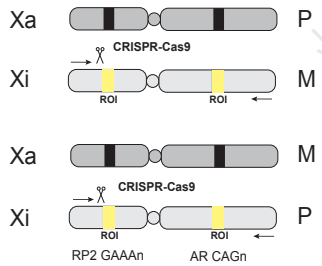
Figure 4 The inactive X chromosome (Xi) reactivation as a therapeutic approach for X-linked disorders. **(A)** Reactivation of Xi-linked methyl-CpG-binding protein 2 (*Mecp2*) in female mouse brain cells using activin A receptor type I (ACVR1) and 3-phosphoinositide-dependent protein kinase 1 (PDPK1) inhibitors. The *Xist:Mecp2-Gfp/Y* male mouse was crossed with *XistΔ:Mecp2/Xist:Mecp2* female mice. This cross generated the *XistΔ:Mecp2/Xist:Mecp2-GFP* mice, where the active X chromosome (Xa) lacks *Xist* and expresses *Mecp2*, while Xi carries the *Mecp2-GFP* reporter and remains silenced. ACVR1 inhibition: LDN193189 blocks ACVR1, a component of the bone morphogenetic protein (BMP) signaling pathway. When ACVR1 is inhibited, Sma- and Mad-related proteins (SMAD) cannot be phosphorylated, preventing them from entering the nucleus and binding to the *Xist* promoter. PDPK1 inhibition: GSK650394 targets PDPK1, which modulates *Xist* RNA localization, stability, and chromatin accessibility. PDPK1 inhibition reduces the expression of *Xist* by preventing its interaction with the Yin Yang 1 (YY1) transcription factor at the *Xist* promoter. This leads to the reactivation of Xi-linked *Mecp2*. The combined treatment of ACVR1 and PDPK1 inhibitors results in a 30% reactivation of Xi-*Mecp2-GFP* expression in female cortical cells. **(B)** Synergistic reactivation of the X-inactive chromosome via DNA demethylation and *Xist*-targeting antisense oligonucleotides. 5-aza-2-deoxycytidine (Aza), a small-molecule inhibitor of DNA methylation, reduces methylation marks on the *Xist* promoter, facilitating the reactivation process. Gapmers1, a specific type of antisense oligonucleotide (ASO), binds to the Repeat A region of *Xist*, utilizing the RNA degradation mechanism mediated by ribonuclease H (RNase H) to selectively degrade *Xist* RNA, thereby promoting the activation of the *Mecp2* gene on the

Xi. In mouse embryonic fibroblasts (MEFs) with a *Mecp2*-luciferase reporter, this combined treatment results in a 2%–5% restoration of normal *Mecp2* levels. (C) Reactivation of Xi-linked *Mecp2* in mouse tail fibroblasts using JAK/STAT inhibitors. Transfected mouse tail fibroblasts carrying the *Mecp2*-luciferase reporter gene located on the Xi were treated with AG490 (a JAK2 inhibitor) or Jaki (a pan JAK/STAT pathway inhibitor). These inhibitors suppress the JAK/STAT signaling pathway. Inhibition of JAK/STAT reduces the expression of *Xist*, thereby reactivating the *Mecp2* gene on the Xi. This leads to an increase in *Mecp2*:luciferase expression. (D) miR106a reactivates the Xi. In the *Tsix*^{ΔCpG^{-/-}}:*Mecp2*^{+/-} mice, the adeno-associated virus serotype 9 (AAV9) vector carrying the miR106a inhibitor miR106a sponge (miR106sp) targets the repeat A region of *Xist* RNA, resulting in decreased *Xist* RNA stability and disruption of N6-methyladenosine (m⁶A) modification and YTH domain-containing 1 (YTHDC1) binding. As a result, the *Mecp2* protein level significantly increases, improving the lifespan, motor coordination, respiratory rhythms, and brain volume in mice.

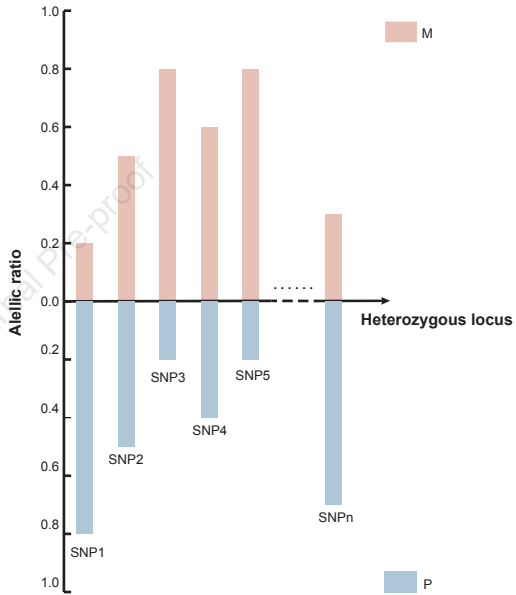


Impact of XCI Skewing on Disease Phenotype

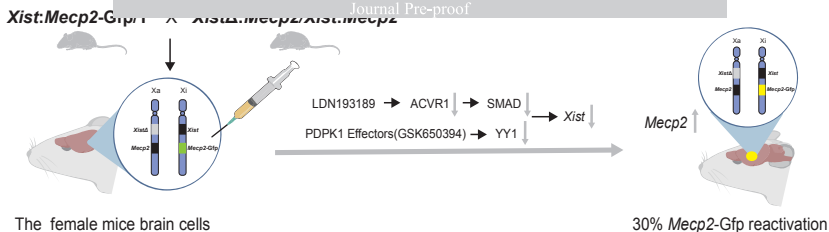


(A)**(B)****(C)**

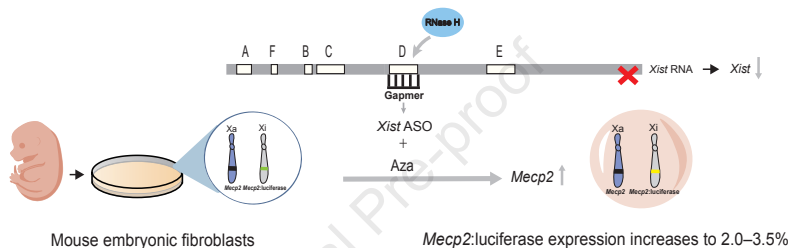
Journal Pre-proof



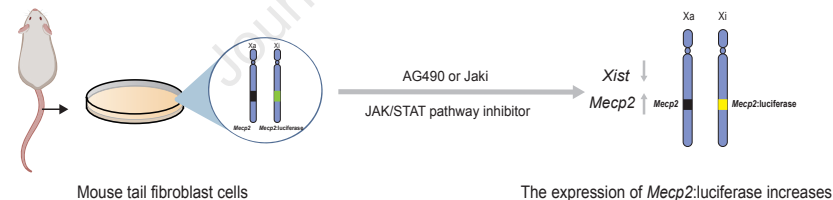
(A)



(B)



(C)



(D)

